Journal of Marine Systems 211 (2020) 103397

Contents lists available at ScienceDirect

Journal of Marine Systems

journal homepage: www.elsevier.com/locate/jmarsys

Future acidification of the Baltic Sea – A sensitivity study

Erik Gustafsson[a,*], Bo G. Gustafsson[a,b]

[a] Baltic Nest Institute, Baltic Sea Centre, Stockholm University, SE-10691 Stockholm, Sweden
[b] Tvärminne Zoological Station, University of Helsinki, J.A. Palménin tie 260, 10900 Hanko, Finland

ARTICLE INFO

Keywords:
Marine carbonate system
Physical-biogeochemical modelling
Sensitivity experiments
Baltic Sea

ABSTRACT

Future acidification of coastal seas will depend not only on the development of atmospheric CO_2 partial pressure (pCO_2), but also on changes in the catchment areas, exchange with the adjacent ocean, and internal cycling of carbon and nutrients. Here we use a coupled physical-biogeochemical Baltic Sea model to quantify the sensitivity of pH to changes both in external forcing and internal processes. The experiments include changes in runoff, supply of dissolved inorganic carbon (DIC) and total alkalinity (A_T), nutrient loads, exchange between the Baltic and North Seas, and atmospheric pCO_2. We furthermore address the potential different future developments of runoff and river loads in boreal and continental catchments, respectively. Changes in atmospheric pCO_2 exert the strongest control on future pH according to our calculations. This CO_2-induced acidification could be further enhanced in the case of desalination of the Baltic Sea, although increased concentrations of A_T in the river runoff due to increased weathering to some extent could counteract acidification. Reduced nutrient loads and productivity would reduce the average annual surface water pH but at the same time slightly increase wintertime surface water pH (the annual pH minimum). The response time of surface water pH to sudden changes in atmospheric pCO_2 is approximately one month, whereas response times to changes in e.g. runoff and A_T/DIC loads are more related to residence times of water and salt (> 30 years). It seems unlikely that the projected future increase in atmospheric pCO_2 and associated pH reduction could be fully counteracted by any of the other processes addressed in our experiments.

1. Introduction

The pH decrease in open ocean surface waters due to increasing atmospheric pCO_2 is quite predictable (e.g. Doney et al., 2009), in contrast to coastal seas where there are no uniform pH trends (Carstensen and Duarte, 2019). The reason is that in coastal seas, pH can change in response to changes in the adjacent catchment. Such processes include changes in precipitation patterns and hydrology, weathering and liming activities in the catchment that can modify the acid buffering capacity (expressed by A_T), and changing nutrient loads and production/respiration patterns. In the open ocean, changes in these processes are normally very slow compared to the rate of CO_2 change, whereas in coastal seas, they can change on approximately the same time-scale as the atmospheric CO_2 level or even faster (Carstensen and Duarte, 2019). This means that pH (and the other parameters of the carbonate system) can be considerably more dynamic and unpredictable in coastal seas than in the open ocean.

The Baltic Sea is a good example of a coastal sea where the above-mentioned processes have indeed been observed to change over the past decades and longer time-scales. Decadal trends in salinity are for example well described based on observations dating back to the late 19th century (Fonselius and Valderrama, 2003; Gustafsson and Stigebrandt, 2007; Mohrholz, 2018). In addition to the natural variability of Baltic Sea salinity dynamics, an overall increase in precipitation and runoff is projected for the coming century as a result of climate change (e.g. Saraiva et al., 2019), resulting in a lower proportion of North Sea water and thus a reduced salinity in the brackish Baltic Sea. A lower proportion of North Sea water would also influence A_T in the Baltic Sea since North Sea water has typical ocean A_T concentrations (~2250 μmol kg^{-1}; see Section 2.3), which is much higher than the average Baltic Sea A_T of approximately 1530 μmol kg^{-1} (calculated by dividing the total A_T pool of ~33,000 Gmol (Gustafsson et al., 2014) by the total water volume of ~21,600 km^3).

For most Swedish rivers, there are monitoring data of water properties and runoff dating back to the early 1970s (Sun et al., 2017). These data show an overall increase in A_T loads to the Baltic Sea decoupled from runoff variations – the flow-normalized A_T loads from Swedish rivers increased by approximately 21% over the period 1985–2012 (Gustafsson et al., 2019a, 2019b). This could be explained by changes in weathering rates or possibly also by liming in the

* Corresponding author.
E-mail address: erik.gustafsson@su.se (E. Gustafsson).

https://doi.org/10.1016/j.jmarsys.2020.103397
Received 23 January 2020; Received in revised form 1 June 2020; Accepted 23 June 2020
Available online 07 July 2020

Table 1
Average values of external forcing parameters in the REF simulation (model run #1): atmospheric pCO_2, Baltic Sea mean air temperature, total runoff, total loads, and ocean boundary concentrations of A_T and DIC.

Parameter	Value	Unit
Atmospheric pCO_2	416	µatm
Air temperature	6.2	°C
River runoff	493	$km^3\ year^{-1}$
A_T land load	810	$Gmol\ year^{-1}$
DIC land load	887	$Gmol\ year^{-1}$
N load (land + atmosphere)	905	$ktons\ year^{-1}$
P load (land + atmosphere)	30	$ktons\ year^{-1}$
Ocean boundary A_T	2250[a]	$\mu mol\ kg^{-1}$
Ocean boundary DIC	2080[a]	$\mu mol\ kg^{-1}$

[a] Computed for salinity = 34 (see text in Section 2.3).

catchments. Such long-term observational time-series are not generally available for other Baltic Sea catchments, but the Swedish data nevertheless give an indication of potential A_T changes related to activities on land. However, based on observations the annual A_T loads from Swedish rivers is on average approximately 42 Gmol (Gustafsson et al., 2019a, 2019b), and thus only a small fraction of the total A_T load to the Baltic Sea (see Table 1).

Human activities on land can also be exemplified by large-scale changes in crop and livestock production and use of industrial fertilizers in Baltic Sea catchments over the past century (and ongoing). This led to a massive increase of nutrient loads to the sea in particular in the period ~1950–1990, followed by a gradual decrease in recent decades primarily as a result of wastewater treatment efforts (Gustafsson et al., 2012). Changes in productivity influence pH both by CO_2 assimilation/respiration and by production and consumption of A_T related to nutrient uptake by primary producers as well as aerobic and anaerobic mineralization processes (e.g. Wolf-Gladrow et al., 2007; Krumins et al., 2013). In stratified water bodies like the Baltic Sea, production and respiration processes can in addition be spatially separated, potentially leading to contrasting pH trends in surface and deep water, respectively (Cai et al., 2011; Carstensen and Duarte, 2019).

Strong horizontal salinity gradients characterize the brackish Baltic Sea, with almost limnic conditions in the far north but in contrast almost oceanic conditions in the entrance area (e.g. Leppäranta and Myrberg, 2009). The Baltic Sea carbonate system is also characterized by large horizontal gradients, partly related to the salinity gradients (proportions of high-A_T North Sea water), but also to river water properties that can differ largely depending on characteristics of the various catchments (Beldowski et al., 2010; see also Section 4.4.1). Such region-dependent carbonate system particularities will be discussed, although our analyses will mainly focus on the Gotland Sea (sub-basin 9, Fig. 1), which is the largest sub-basin of the Baltic Sea and representative for central Baltic or Baltic Proper conditions.

Projections of future pH, A_T, and oxygen concentrations in the Baltic Sea have been explored for specific scenarios by Omstedt et al. (2012), including the impacts of land-use and nutrient load changes as well as climate change. It can however be challenging to separate effects related to changes in freshwater balance and temperature, changes in nutrient loads and productivity, changes in atmospheric pCO_2, and changes in weathering rates – processes that typically change simultaneously but more or less independently. In the present study, the factors that influence pH in the Baltic Sea will be examined by means of sensitivity experiments using the process-based BALTSEM model (see Section 2.1). Our main objectives are to 1. identify key processes that control pH in the Baltic Sea, 2. quantify possible future pH change and range, and 3. discuss pH sensitivity and also response times to changes in the processes that control pH.

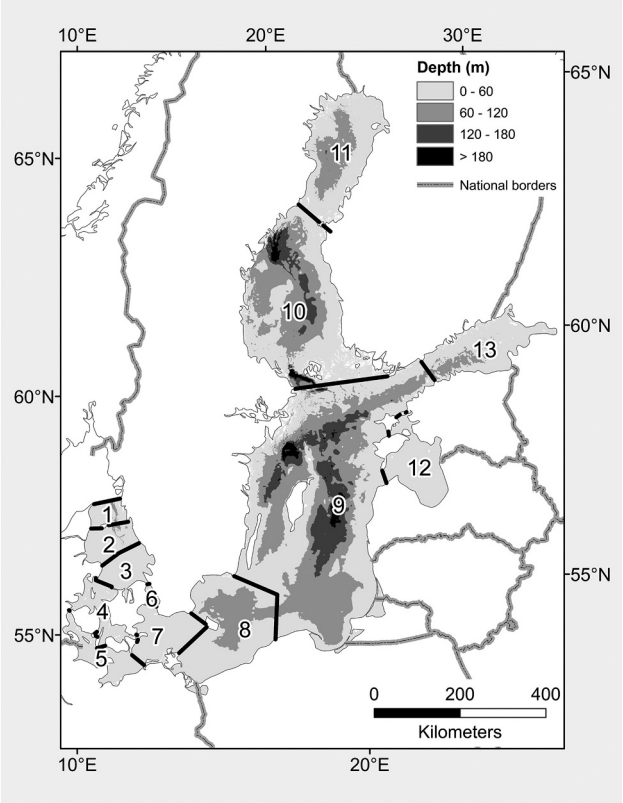

Fig. 1. Sub-basin division of the Baltic Sea in BALTSEM: 1. Northern Kattegat (NK), 2. Central Kattegat (CK), 3. Southern Kattegat (SK), 4. Samsø Belt (SB), 5. Fehmarn Belt (FB), 6. Öresund (OS), 7. Arkona Basin (AR), 8. Bornholm Basin (BN), 9. Gotland Sea (GS), 10. Bothnian Sea (BS), 11. Bothnian Bay (BB), 12. Gulf of Riga (GR), 13. Gulf of Finland (GF).

2. Material and methods

In this section, we describe first the model used for our analyses (Section 2.1), followed by a description of how the model simulations were constructed (Section 2.2), then a description of a reference model simulation (to which the other sensitivity experiments will be compared) (Section 2.3), and finally a description of how the different pH influencing factors will be addressed by means of sensitivity experiments (Sections 2.4–2.5).

2.1. The BALTSEM model

BALTSEM (Baltic Sea long-term large-scale eutrophication model) is a coupled physical-biogeochemical model employing a basin-scale approach with 13 different sub-basins that are described as horizontally homogenous but with a vertical resolution of approximately 1 m (Fig. 1). The model has been described and thoroughly validated in numerous publications, focusing on e.g. physical processes (Gustafsson, 2000, 2003), eutrophication, nutrient cycling, and oxygen dynamics (Gustafsson et al., 2012, 2017; Savchuk et al., 2012; Meier et al., 2018; Murray et al., 2019), or the carbonate system (Gustafsson et al., 2014, 2015, 2019a, 2019b). BALTSEM has been demonstrated to reasonably well reproduce observed salinity, temperature, oxygen and nutrient concentrations, as well as productivity patterns (Gustafsson et al., 2012, 2017; Savchuk et al., 2012), and also carbonate system parameters such as pH and A_T (Gustafsson, 2013; Gustafsson et al., 2015, 2019a, 2019b). In particular, detailed comparisons between observed and simulated

carbonate system parameters are included in Gustafsson (2013), whereas comparisons between simulated and observed A_T in surface and deep water of major Baltic Sea sub-basins are shown in Gustafsson et al. (2019a, 2019b).

BALTSEM simulates salinity, temperature, dissolved oxygen, dissolved inorganic and organic nutrients and carbon, detrital nutrients and carbon, A_T, three phytoplankton groups, and one bulk state variable for the heterotroph community. Model state variables are listed in Table A1 (Appendix A1). Cycling of carbon and nutrients is illustrated in Fig. A1 (Appendix A1). The carbonate system can be characterized by four parameters; DIC, A_T, hydrogen ion concentration (expressed as pH), and pCO_2. If two of these parameters are known (in our case DIC and A_T), the other two can be calculated. A brief description of these four variables is available in Appendix A2 (detailed descriptions are available in e.g. Dickson et al. (2007)). Most biogeochemical processes related to pelagic and sedimentary cycling of N, P, and sulfur (S) either consume or produce A_T. The stoichiometry of primary production and mineralization processes – and the impact on A_T – is listed in Table A2 (Appendix A3).

2.2. Experimental setup

As mentioned in the introduction, pH can change because of other processes than just the CO_2 effect, leading to non-uniform and unpredictable long-term pH trends in coastal seas (Carstensen and Duarte, 2019). One main incentive for the different sensitivity experiments in this study is to single out just one or a couple of pH influencing factors at the time, and then to quantify the associated pH sensitivity. Model settings for the sensitivity experiments are described in Section 2.2.1.

All model simulations were run over a period of 300 years: the first 200 years were used as spin-up time so that the results presented in Sections 3–4 are from the last 100 years of the various simulations. The residence time for water and salt is approximately 35 years (Stigebrandt and Gustafsson, 2003), whereas the residence times for nitrogen (N) and phosphorus (P) are approximately 10 and 50 years respectively (Gustafsson et al., 2017). Using a 200-year spin-up time thus means that the model has reached a quasi-steady state (only "quasi" since there is a natural variability in the physical forcing, see Section 2.2.1).

2.2.1. Sensitivity experiments

In these scenarios we use non-climate change statistical forcing data for atmospheric conditions, river runoff, and boundary conditions. This means that it will be possible to address the impacts of e.g. different nutrient loads or atmospheric pCO_2 levels without simultaneously accounting for the impact of climate change (i.e., changes in temperature, precipitation patterns, etc.). To this end, a set of 11 different scenarios with non-climate change statistical forcing was constructed:

The statistical forcing was based on reconstructed forcing for the period 1850–2006 (Gustafsson et al., 2012) in order to simulate a natural variability of physical drivers. These original time-series were as a first step sliced, and these slices were then put together by random selection (but originating from the same time of the year within a 3-month interval). In order to avoid unrealistic sea level jumps, the original time-series were sliced at each instance of zero sea level at the open ocean boundary. The method used to construct forcing files for our 11 non-climate change scenarios has previously been described by Ehrnsten et al. (2020). At the open ocean boundary, the same concentration for each model state variable was repeated each year, but with a seasonality based on observations in the period 1980–2006. Furthermore, there are no long-term trends in the external loads of nutrients, carbon, and A_T in these scenarios. Instead we use constant riverine A_T and DIC (see Section 2.3), and a constant atmospheric deposition of oxidized sulfur (an A_T sink) based on data by Claremar and Rutgersson (2017). We also use constant land loads and atmospheric depositions of inorganic and organic N and P constituents, as well as land loads of dissolved silica.

2.3. Reference model simulation

In the reference model simulation (REF), we use the physical forcing (including e.g. weather data and river runoff) from one specific realization of the non-climate change scenarios described in Section 2.2.1. The sensitivity model simulations described in Section 2.4 will be compared to this REF simulation.

At the Barrow Station in Alaska, the annual mean atmospheric pCO_2 was approximately 410 μatm as of 2018 (Barrow Atmospheric Baseline Observatory data, https://www.esrl.noaa.gov/gmd/obop/brw/). In the Baltic Sea area, the atmospheric pCO_2 is similar to that observed at Barrow Station, but on average about 3 μatm higher (Schneider, 2011). Furthermore, the contemporary increase in atmospheric pCO_2 is approximately 2 μatm per year. For those reasons, we use an atmospheric pCO_2 of about 416 μatm (present-day Baltic Sea mean) throughout the REF simulation.

Constant seasonal cycles are used for concentration profiles at the ocean boundary as described in Section 2.2.1. Concentrations of A_T and DIC at the boundary are calculated as functions of salinity (salinity at the ocean boundary varies depending on season and depth) according to $A_T = 27 * \text{salinity} + 1330$ (μmol kg^{-1}) and $DIC = 27 * \text{salinity} + 1160$ (μmol kg^{-1}). These linear relations were found by model calibration calculations (Gustafsson, 2013). A comparison between simulated and observed concentrations is indicated in Fig. S1 (Supporting information).

All external loads are kept at uniform levels throughout the simulation (i.e., no trends over time). Supplies (land loads + atmospheric depositions) of N and P respectively are average loads from the period 2012–2014 (HELCOM, 2018). Land loads of A_T and DIC are based on observations in the period 1996–2000 (see Table S1 in the Supporting information of Gustafsson et al. (2015)). However, these loads are not sufficient to reproduce observed A_T and DIC in the Baltic Sea. For that reason, Gustafsson et al. (2019b) calibrated the so called "unresolved A_T sources" (that could represent unknown/underestimated riverine sources and/or unresolved biogeochemical processes) that were necessary to reproduce observed A_T (see Table 5 in Gustafsson et al., 2019b). In the present study we shall for simplicity assume that all of the unresolved A_T sources are in the form of underestimated river loads (although Gustafsson et al. (2019b) estimated that up to 18% of the unresolved source in the Baltic Proper could be a result of pyrite burial, a process that is not included in BALTSEM). Since both A_T and DIC largely consist of bicarbonate, we also add an equally large additional riverine source of DIC. The average land loads of A_T and DIC as well as other forcing parameters used in the REF simulation are indicated in Table 1.

2.4. Factors addressed in the sensitivity experiments

Here follows a description of the different factors addressed in the sensitivity experiments. The modifications in these simulations compared to the REF simulation are summarized in Table 2.

2.4.1. Atmospheric pCO_2

In these experiments, we shall examine the differences in pH when forcing the model with either pre-industrial (280 μatm) or present-day pCO_2 (416 μatm) throughout the model simulations. We shall further examine the CO_2-induced pH change by forcing the model with either 550 or 950 μatm atmospheric pCO_2. These are the approximate values of atmospheric pCO_2 by the year 2100 if either the RCP (Representative

Table 2
Average values of the external forcing parameters that are modified in the different sensitivity experiments (see also text in Section 2.4).

Model run	Factor addressed	Case	Value	Unit
#2	Atmospheric pCO_2	Pre-industrial	280	μatm
#3	Atmospheric pCO_2	RCP 5.5, year 2100	550	μatm
#4	Atmospheric pCO_2	RCP 8.5, year 2100	950	μatm
#5	Air temperature	REF − 1 °C	5.2	°C
#6	Air temperature	REF − 2 °C	4.2	°C
#7	Air temperature	REF + 1 °C	7.2	°C
#8	Air temperature	REF + 2 °C	8.2	°C
#9	River runoff	REF − 10%	444	$km^3\ year^{-1}$
#10	River runoff	REF − 20%	395	$km^3\ year^{-1}$
#11	River runoff	REF + 10%	543	$km^3\ year^{-1}$
#12	River runoff	REF + 20%	592	$km^3\ year^{-1}$
#13	A_T/DIC land loads	REF − 10%	729/798	$Gmol\ year^{-1}$
#14	A_T/DIC land loads	REF − 20%	648/710	$Gmol\ year^{-1}$
#15	A_T/DIC land loads	REF + 10%	891/976	$Gmol\ year^{-1}$
#16	A_T/DIC land loads	REF + 20%	972/1064	$Gmol\ year^{-1}$
#17	N/P loads (land + atm.)	BSAP	796/20	$ktons\ year^{-1}$
#18	N/P loads (land + atm.)	HEL	1050/37	$ktons\ year^{-1}$
#19	N/P loads (land + atm.)	HIGH	1330/68	$ktons\ year^{-1}$
#20	Ocean boundary A_T/DIC	REF − 10%	2020/1870[a]	$\mu mol\ kg^{-1}$
#21	Ocean boundary A_T/DIC	REF − 20%	1800/1660[a]	$\mu mol\ kg^{-1}$
#22	Ocean boundary A_T/DIC	REF + 10%	2470/2290[a]	$\mu mol\ kg^{-1}$
#23	Ocean boundary A_T/DIC	REF + 20%	2700/2490[a]	$\mu mol\ kg^{-1}$
#24	Runoff, A_T/DIC loads	REF − 10%	444, 729/798	$km^3\ year^{-1}$, $Gmol\ year^{-1}$
#25	Runoff, A_T/DIC loads	REF − 20%	395, 648/710	$km^3\ year^{-1}$, $Gmol\ year^{-1}$
#26	Runoff, A_T/DIC loads	REF + 10%	543, 891/976	$km^3\ year^{-1}$, $Gmol\ year^{-1}$
#27	Runoff, A_T/DIC loads	REF + 20%	592, 972/1064	$km^3\ year^{-1}$, $Gmol\ year^{-1}$
#28	DIC land loads	REF − 10%	798	$Gmol\ year^{-1}$
#29	DIC land loads	REF − 20%	710	$Gmol\ year^{-1}$
#30	DIC land loads	REF + 10%	976	$Gmol\ year^{-1}$
#31	DIC land loads	REF + 20%	1064	$Gmol\ year^{-1}$
#32	Runoff, A_T/DIC land loads	BS, BB + 10%; BN, GS, GR − 10%	498, 759/837	$km^3\ year^{-1}$, $Gmol\ year^{-1}$
#33	Runoff, A_T/DIC land loads	BS, BB + 20%; BN, GS, GR − 20%	502, 708/788	$km^3\ year^{-1}$, $Gmol\ year^{-1}$
#34	A_T/DIC land loads	BS, BB + 10%; BN, GS, GR − 10%	759/837	$Gmol\ year^{-1}$
#35	A_T/DIC land loads	BS, BB + 20%; BN, GS, GR − 20%	708/788	$Gmol\ year^{-1}$

[a] Computed for salinity = 34 (see text in Section 2.3).

Concentration Pathways) 4.5 or RCP 8.5 scenario, respectively, are realized (van Vuuren et al., 2011).

2.4.2. Air temperature

In these experiments, the air temperatures used in the REF simulation will be modified by −1 °C, −2 °C, +1 °C, or +2 °C, with no other changes in atmospheric forcing.

2.4.3. Runoff

In these experiments, the river runoff used in the REF simulation will be modified by −10%, −20%, +10%, or +20%, without changing the land loads of nutrients, DIC, and A_T. Thus, in this scenario we only examine the consequences of changing the freshwater balance, or in other words the relative proportion of North Sea water in the Baltic Sea. The runoff changes are here modelled as uniform for all Baltic Sea catchments.

2.4.4. External supply of DIC and A_T

In these experiments, the land loads of DIC and A_T used in the REF simulation will be modified by −10%, −20%, +10%, or +20% without corresponding changes in runoff. These scenarios would thus correspond to changes in riverine concentrations of A_T and DIC induced for example by changes in weathering rates (see Section 4.4).

2.4.5. Runoff and external supply of DIC and A_T

In these experiments, the river runoff and land loads of DIC and A_T used in the REF simulation will be modified by −10%, −20%, +10%, or +20%. These scenarios would thus correspond to changes in river runoff, but keeping the riverine concentrations of A_T and DIC constant.

2.4.6. North-south gradients in precipitation patterns

In these experiments, the runoff and also the land loads of A_T and DIC to the Bothnian Sea and Bothnian Bay (BS and BB, see Fig. 1) will be increased by either 10 or 20%, but at the same time the runoff and A_T and DIC loads to the Bornholm Basin (BN), the Gotland Sea (GS), and the Gulf of Riga (GR) will be decreased by either 10 or 20%. The purpose is to examine the potential pH change related to contrasting future precipitation trends in northern and southern parts of the Baltic Sea (see further discussion in Section 4.4.1). In order to distinguish the effect of modified A_T and DIC supplies from the salinity effect (by changing runoff), two additional sensitivity experiments will be performed where only the land loads of A_T and DIC to these sub-basins will be changed without corresponding changes in runoff.

2.4.7. Nutrient loads

In these experiments, the land loads of N and P used in the REF simulation will be modified without corresponding changes in runoff. In the REF simulation, the N and P loads are based on observations from 2012 to 2014 as described above (Section 2.3). That scenario shall be compared to simulations where we use either 1. the maximum allowable loads according to the Baltic Sea Action Plan (BSAP), which are the desired future N and P loads that could eventually restore the Baltic Sea to a state unaffected by eutrophication issues (HELCOM, 2013), or 2. average loads based on observations in the period 1997–2003 (HEL), which is a reference period often referred to in the context of recent nutrient load reductions (HELCOM, 2015), or finally 3. average loads

from 1980 to 1990 (HIGH) which is the period when loads to the Baltic Sea peaked (Gustafsson et al., 2012).

2.4.8. Concentrations at the ocean boundary

In these experiments, the ocean boundary concentrations of DIC and A_T used in the REF simulation will be modified by −10%, −20%, +10%, or +20% without corresponding changes in salinity. Such changes could in theory be related to changes in the oceanic soft-tissue and carbonate pumps (see Section 4.6).

2.5. Response times

In these experiments, we investigate the time it takes for the carbonate system parameters to respond and adjust to changes in model forcing by first running the REF scenario for 200 years, then instantaneously changing one forcing factor and running the model for another 100 years (keeping the adjusted forcing throughout the model run). This means that the response time experiments presented below (Section 4.7) all start from identical initial conditions, and in addition at a point in time where the model has reached a quasi-steady state (as discussed in Section 2.2). The factors addressed here will be:

1. Instantaneous change from pCO_2 in the REF simulation (Table 1) to pCO_2 values in either the pre-industrial or RCP 8.5 simulations, respectively (Table 2).
2. Instantaneous increase in runoff by either 10 or 20% compared to the REF simulation.
3. Instantaneous increase in land loads of A_T and DIC by either 10 or 20% compared to the REF simulation.
4. Instantaneous change from nutrient loads in the REF simulation to nutrient loads in either the BSAP or HIGH simulations, respectively (Table 2).
5. Instantaneous increase in A_T and DIC concentrations at the ocean boundary by either 10 or 20% compared to the REF simulation.

3. Results

3.1. "Natural" variability

The "natural" variability in terms of e.g. salinity, temperature, and carbonate system parameters is addressed by comparing the 11 different non-climate change scenarios (described in Section 2.2.1). Fig. 2 indicates average properties in Gotland Sea surface water based on the last 100 years of these simulations. The standard deviations in Fig. 2 indicate differences between annual average time-series of the different scenarios (seasonal variations are typically very large compared to inter-annual variations, see Fig. 3). From these 11 scenarios, we find the following average properties for Gotland Sea surface water: salinity = 6.82 ± 0.09, temperature = 7.33 ± 0.06 (°C), A_T = 1559 ± 9.8 (μmol kg^{-1}), DIC = 1515 ± 9.2 (μmol kg^{-1}), pCO_2 = 419.6 ± 0.50 (μatm), and pH = 8.00 ± 0.002.

3.2. Reference model simulation

One of the non-climate change scenarios was used for the REF simulation. In this scenario, the average surface water A_T and DIC concentrations (1560 and 1516 respectively, see Table 3) are very similar to the average concentrations based on all 11 scenarios described in Sections 2.2.1 and 3.1.

Fig. 4 illustrates the differing surface water properties between different sub-basins of the system according to the REF simulation. Particularly noteworthy here are the large differences in e.g. A_T concentrations in the Bothnian Sea, the Gulf of Riga, and the Gulf of Finland (GF, see Fig. 1) in spite of similar salinities – a result of different river water properties related to bedrock characteristics of the catchments, i.e., granite or limestone dominated (see e.g. Beldowski et al., 2010). We also observe considerable differences in pH and DIC levels between the different sub-basins – a consequence of A_T concentrations (see further discussions in Section 4.4). The seasonal developments of pCO_2 and pH in the different sub-basins reflect wintertime nutrient concentrations and productivity (i.e., CO_2 uptake) (see further discussions in Section 4.5).

3.3. Sensitivity experiments

Here we present results from the sensitivity experiments described in Section 2.4, i.e., the experiments addressing changes in only one pH-influencing parameter at a time. Table 3 shows average salinity, A_T and DIC concentrations, and pH in Gotland Sea surface water. Results are presented first from the REF simulation (Section 2.3) and then from the

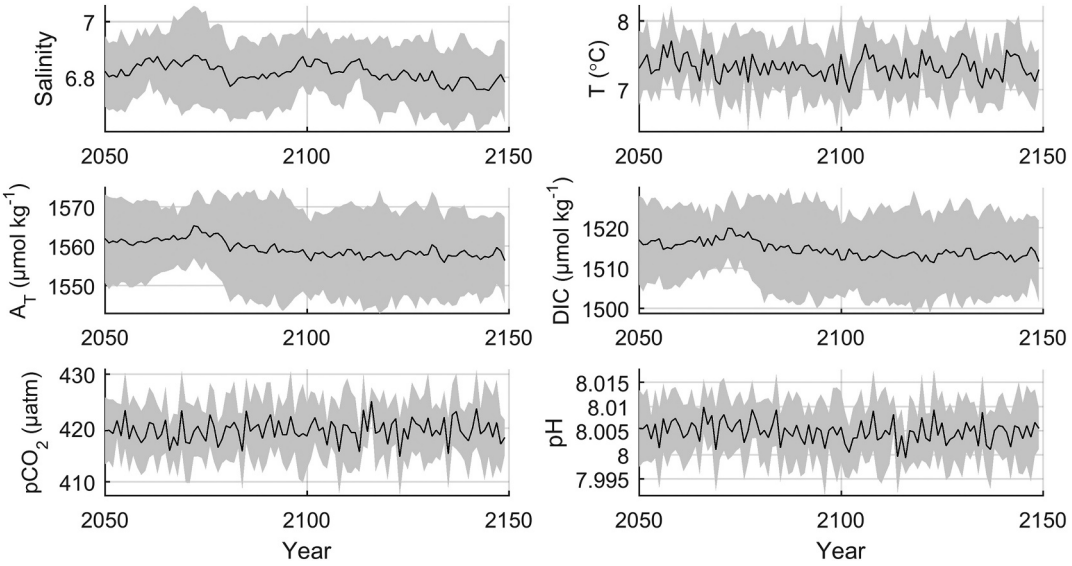

Fig. 2. Simulated salinity, temperature, A_T, DIC, pCO_2, and pH in the Gotland Sea surface water indicating annual average values (black lines) ± standard deviation of these annual averages (shaded areas) from the last 100 years of the different statistical forcing scenarios (see Section 2.2.1).

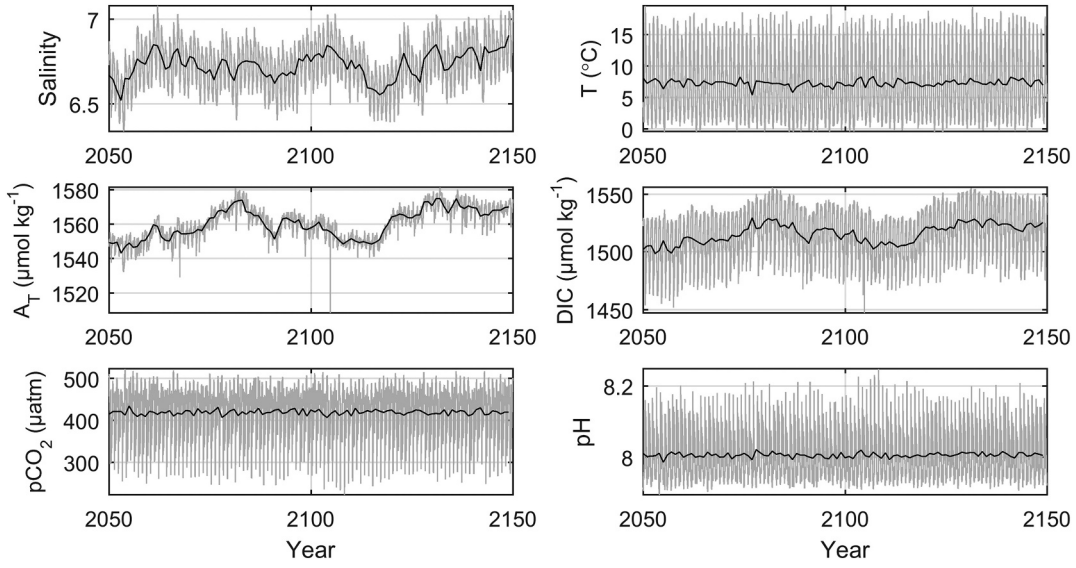

Fig. 3. Simulated salinity, temperature (°C), A_T (µmol kg^{-1}), DIC (µmol kg^{-1}), pCO_2 (µatm), and pH in Gotland Sea surface water (from the last 100 years of the REF simulation, see Section 2.3), showing model output every 5 days (gray), and annual average values (black) respectively.

Table 3
Average values of Gotland Sea surface water salinity, temperature, DIC (µmol kg^{-1}), A_T (µmol kg^{-1}), pCO_2 (µatm), and pH in different sensitivity experiments (Section 2.4) as well as the pH difference (ΔpH) between the REF simulation (Section 2.3) and the sensitivity experiments (comparing average values from the last 100 years of the respective simulations). A sense of the order of magnitude of the pH change can be obtained by comparing with the estimated long-term variability of ± 0.002 derived in Section 3.1.

Run	Factor addressed	Case	Salinity	T	A_T	DIC	pCO_2	pH	ΔpH
#1	None	REF simulation	6.73	7.31	1560	1516	419.9	8.01	NA
#2	Atmospheric pCO_2	Pre-industrial	6.73	7.31	1560	1491	287.1	8.16	0.16
#3	Atmospheric pCO_2	RCP 5.5, year 2100	6.73	7.31	1560	1534	552.4	7.89	−0.11
#4	Atmospheric pCO_2	RCP 8.5, year 2100	6.73	7.31	1560	1573	952.1	7.66	−0.35
#5	Air temperature	REF − 1 °C	6.53	6.44	1544	1504	421.6	8.00	−0.01
#6	Air temperature	REF − 2 °C	6.22	5.64	1522	1486	426.9	7.99	−0.01
#7	Air temperature	REF + 1 °C	6.86	8.18	1573	1524	419.1	8.01	0.00
#8	Air temperature	REF + 2 °C	6.95	9.06	1583	1531	418.6	8.02	0.01
#9	River runoff	REF − 10%	7.57	7.32	1678	1626	420.3	7.99	0.02
#10	River runoff	REF − 20%	8.51	7.33	1808	1747	420.8	8.01	0.04
#11	River runoff	REF + 10%	5.98	7.30	1455	1416	419.0	7.96	−0.02
#12	River runoff	REF + 20%	5.32	7.29	1359	1326	418.5	7.94	−0.03
#13	A_T/DIC land loads	REF − 10%	6.73	7.31	1449	1410	418.6	7.95	−0.03
#14	A_T/DIC land loads	REF − 20%	6.73	7.31	1339	1303	417.2	7.91	−0.06
#15	A_T/DIC land loads	REF + 10%	6.73	7.31	1671	1622	421.3	8.00	0.03
#16	A_T/DIC land loads	REF + 20%	6.73	7.31	1782	1727	422.7	8.02	0.05
#17	N/P loads (land + atm.)	BSAP	6.73	7.31	1557	1517	425.2	7.97	−0.01
#18	N/P loads (land + atm.)	HEL	6.73	7.31	1562	1514	416.0	7.98	0.01
#19	N/P loads (land + atm.)	HIGH	6.73	7.31	1566	1500	396.2	8.03	0.05
#20	Ocean A_T/DIC	REF − 10%	6.73	7.31	1516	1473	419.6	7.96	−0.01
#21	Ocean A_T/DIC	REF − 20%	6.73	7.31	1472	1431	419.3	7.95	−0.02
#22	Ocean A_T/DIC	REF + 10%	6.73	7.31	1605	1558	420.2	7.99	0.01
#23	Ocean A_T/DIC	REF + 20%	6.73	7.31	1649	1601	420.6	8.00	0.02
#24	Runoff, A_T/DIC land loads	REF − 10%	7.57	7.32	1561	1514	418.7	8.00	−0.01
#25	Runoff, A_T/DIC land loads	REF − 20%	8.51	7.33	1561	1512	417.4	7.99	−0.02
#26	Runoff, A_T/DIC land loads	REF + 10%	5.98	7.30	1560	1517	420.3	8.02	0.01
#27	Runoff, A_T/DIC land loads	REF + 20%	5.32	7.29	1559	1519	420.9	8.03	0.02
#28	DIC land loads	REF − 10%	6.73	7.31	1560	1515	414.8	8.01	0.01
#29	DIC land loads	REF − 20%	6.73	7.31	1560	1514	409.7	8.02	0.01
#30	DIC land loads	REF + 10%	6.73	7.31	1560	1517	425.0	8.00	−0.01
#31	DIC land loads	REF + 20%	6.73	7.31	1560	1517	430.1	8.00	−0.01
#32	Runoff, A_T/DIC land loads	BS, BB + 10%; BN, GS, GR − 10%	6.65	7.31	1477	1436	418.4	7.99	−0.02
#33	Runoff, A_T/DIC land loads	BS, BB + 20%; BN, GS, GR − 20%	6.57	7.30	1394	1357	416.8	7.96	−0.04
#34	A_T/DIC land loads	BS, BB + 10%; BN, GS, GR − 10%	6.73	7.31	1488	1447	419.0	7.99	−0.02
#35	A_T/DIC land loads	BS, BB + 20%; BN, GS, GR − 20%	6.73	7.31	1416	1377	418.0	7.97	−0.04

various sensitivity experiments, indicating also the differences in pH between the REF simulation and the various sensitivity experiments.

Compared to the REF simulation, the largest long-term mean pH increase in Gotland Sea surface water occurs in the case where we use pre-industrial instead of present-day atmospheric pCO_2 (ΔpH = +0.16). The largest pH reduction (ΔpH = −0.35) occurs in the case where the atmospheric pCO_2 is on average 950 µatm – more than a doubling of the present-day value. The long-term pH response to a modified temperature by ± 1–2 °C is small (ΔpH = ± 0.01), whereas a larger effect is seen from changes in runoff by ± 10–20%

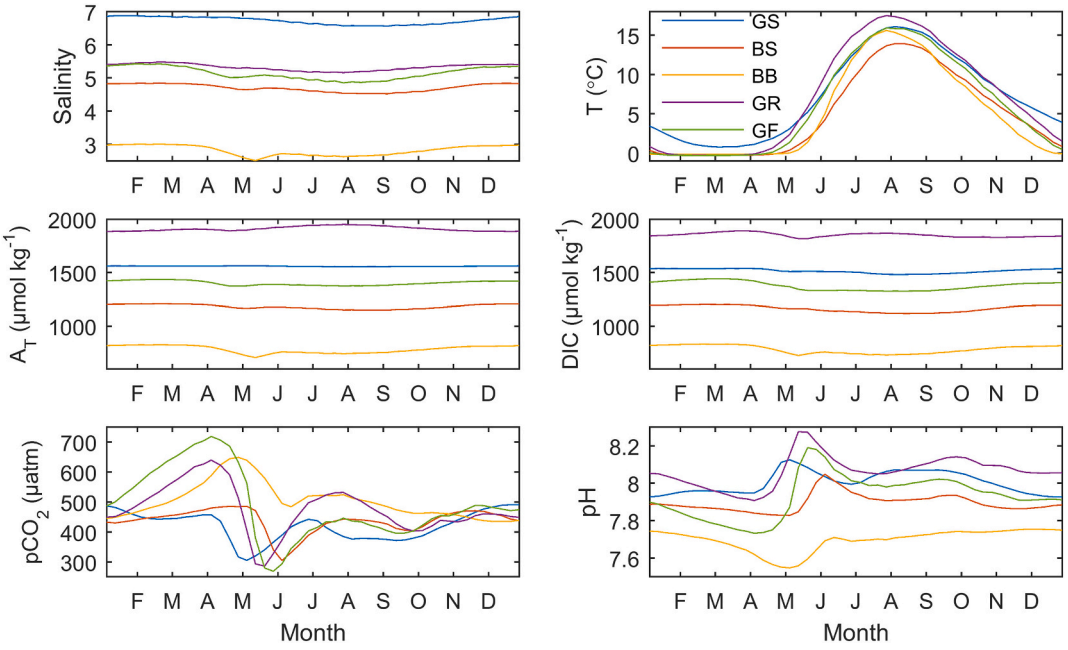

Fig. 4. Average seasonal developments of surface water salinity, temperature (°C), A_T (µmol kg^{-1}), DIC (µmol kg^{-1}), pCO_2 (µatm), and pH in the Gotland Sea (GS), the Bothnian Sea (BS), the Bothnian Bay (BB), the Gulf of Riga (GR), and the Gulf of Finland (GF) in the REF simulation.

(ΔpH = ± 0.02–0.04). Changes in the riverine A_T and DIC concentrations by ± 10–20% result in pH changes in a range ΔpH = ± 0.02–0.06, whereas changes in oceanic A_T and DIC concentrations by ± 10–20% result in a comparatively small pH change (ΔpH = ± 0.01–0.02). In the BSAP case, with reduced nutrient loads, the long-term mean pH in Gotland Sea surface water is marginally smaller than in the REF case (ΔpH = −0.01), whereas in the HIGH case with substantially larger nutrient loads than in REF, the annual mean pH is enhanced by 0.05 units compared to REF. The results and their implications are further discussed in Sections 4.2–4.7.

4. Discussion

4.1. Uncertainties associated with the modelling approach

There are two main sources of uncertainty in our model simulations of carbonate system parameters: 1. The description of biogeochemical processes, and 2. The magnitudes of external sources.

When it comes to biogeochemical processes, there are a couple of known problems related to productivity and CO_2 assimilation. Based on comparisons with observations, the simulated net production appears to be underestimated (particularly in the northern sub-basins but also in the Baltic Proper) in spite of observed wintertime nutrient concentrations being well reproduced by the model (Savchuk et al., 2012). This can at least partly be explained by an underutilization of bioavailable nutrients above the permanent halocline (Eilola et al., 2011). Underutilized nutrient assimilation is also reflected by an underestimated pCO_2 drawdown and underestimated pH increase in the surface layer during the productive season (Gustafsson et al., 2015). BALTSEM includes a 20% excessive CO_2 uptake by autotrophs (compared to cellular C:N:P ratios), but the model still fails to reproduce the observed range of seasonal pCO_2 and pH variations in the surface layer (Gustafsson et al., 2015). Model experiments indicate that the seasonality of pCO_2 and pH can be improved if a flexible cell stoichiometry for the autotrophs is allowed (Kreus et al., 2015; Fransner et al., 2018), but this is for the time being not an option in BALTSEM where autotrophs instead have fixed cellular C:N:P ratios.

As described in Section 2.3, the A_T sources (external and internal) that are required to reproduce observed A_T concentrations in the Baltic Sea are not fully understood. In this study we included the calibrated unresolved A_T sources by Gustafsson et al. (2019b) as additional river loads, although a fraction of the unresolved source could be a result of pyrite burial (Gustafsson et al., 2019a, 2019b). Another open question is the possible contribution from submarine groundwater discharge (Gustafsson et al., 2014). As discussed in some detail below (Section 4.5.1), there is over longer time-scales an upper limit for A_T generation coupled to nutrient cycling (although short-term variations could be comparatively large depending on variations in the hypoxic and anoxic bottom areas). It would thus appear reasonable to assume that underestimated/unknown external A_T sources rather than internal generation comprise the main bulk of the unresolved A_T source.

What is also worth emphasizing here is that the results are from one model only. BALTSEM has been compared to other coupled physical-biogeochemical Baltic Sea models in prior studies (Eilola et al., 2011; Meier et al., 2018), but these comparisons did not include the carbonate system.

4.2. Atmospheric pCO_2

In this “pure” ocean acidification case (i.e., pH being changed only by changing the atmospheric pCO_2), the pH response to changing atmospheric pCO_2 (model experiments #2–4, Table 2) is indeed predictable. Using the mean surface water temperature, salinity, A_T (see Table 3), and the average atmospheric pCO_2 values from the different scenarios (see Table 2), the resulting mean surface water pH could be computed directly. Nevertheless, it is in these scenarios that we find the largest shifts in mean pH levels.

The main mechanism of oceanic CO_2 uptake is the reaction of CO_2 with $CO_3^{=}$, forming HCO_3^{-} ($CO_3^{=} + CO_2 + H_2O \rightarrow 2HCO_3^{-}$) (e.g. Schneider, 2011). A gradual increase in atmospheric pCO_2 and oceanic

CO_2 uptake results in reduced $CO_3^{=}$ concentration and thus reduced saturation states of calcium carbonate ($CaCO_3$) minerals (Feely et al., 2004). In the BALTSEM model, this mechanism is not taken into account, the reason being that planktonic calcifiers are believed to be largely absent from the Baltic Sea due to undersaturation of $CaCO_3$ minerals in spring (Tyrrell et al., 2008). It is however worth noting that changes in atmospheric pCO_2 could influence not only DIC and pH, but also A_T by changes in $CaCO_3$ formation/dissolution rates.

4.3. Air temperature

For many reasons, a change in air temperature produces complex responses of carbonate system parameters (and also other quantities). Temperature influences for example the extension of sea ice, or in other words the areas of different sub-basins that in winter are covered by a lid that prevents gas exchange between air and sea. Temperature also controls gas solubility, which on one hand has an impact on air-sea exchange of both CO_2 and O_2. On the other hand, a modified O_2 solubility will also subsequently modify deep water O_2 and also nutrient concentrations since nutrient cycling is to some degree controlled by O_2 concentration. Deep water O_2 also depends on mineralization rates of organic material – rates that are temperature dependent as well. Modified nutrient concentrations will affect the magnitude of plankton blooms. Furthermore, the timing and rates of plankton blooms are temperature dependent as well which means that a modified temperature will change the seasonal development of e.g. carbonate system parameters. For a comprehensive description of how temperature can influence the cycling of nutrients and plankton, and furthermore how the O_2 concentration controls nutrient cycling, the reader is referred to Savchuk (2002).

Nevertheless, we find that the overall effect on pH by changing the temperature by 1 or 2 degrees (model experiments #5–8, Table 2) is comparatively small (approximately ± 0.01 pH units, see Table 3), at least in the long-term perspective employed here. For that reason, we shall not attempt to disentangle the individual pH responses to the various temperature related changes in the system as outlined above.

4.4. Runoff change versus A_T and DIC load change

Changing only the runoff but not the river loads of e.g. A_T and DIC (model experiments #9–12, Table 2) can be interpreted as a case where increased or decreased runoff is compensated by either dilution or increased concentrations, respectively, of the riverborne constituents. On the other hand, changing the loads of A_T and DIC without corresponding changes in runoff (model experiments #13–16, Table 2) would in contrast indicate modified riverine concentrations of A_T and DIC. In the sensitivity experiments where riverine concentrations of A_T and DIC change by the same amounts, the change could be interpreted as a result of changes in the H_2CO_3 driven weathering. Weathering driven by H_2CO_3 (produced by mineralization of soil organic carbon) produces bicarbonate in the cases of H_2CO_3 reacting with both silicate minerals (that typically dominate the boreal, northern catchments of the Baltic Sea) and carbonate minerals (that dominate the continental, southern Baltic Sea catchments, cf. Müller et al. (2016)). Changes in bicarbonate concentration affects A_T and DIC by exactly the same amounts (see Appendix A2).

Changing both runoff and land loads of A_T and DIC (model experiments #24–27, Table 2) – which would correspond to changing the runoff but keeping the riverine A_T and DIC concentrations constant – we have a case of competing effects on the carbonate system parameters: If for example the runoff and loads increase, the increased supply of A_T and DIC would on one hand tend to increase the concentrations. But, on the other hand, there is also the "salinity effect",

Table 4
DIC land load and net air-sea CO_2 exchange (F_{CO2}) (Gmol year^{-1}) on Baltic Sea system-scale in a few selected scenarios (negative F_{CO2} indicates net outgassing and vice versa).

Model run	Factor addressed	Case	DIC land load	F_{CO2}
#1	None	REF	887	−95
#28	DIC loads	REF − 10%	798	−6
#29	DIC loads	REF − 20%	710	83
#30	DIC loads	REF + 10%	976	−184
#31	DIC loads	REF + 20%	1064	−273
#17	N/P loads (land + atm.)	BSAP	887	−139
#18	N/P loads (land + atm.)	HEL	887	−58
#19	N/P loads (land + atm.)	HIGH	887	75

i.e., a reduced proportion of high-salinity and high-A_T ocean water that would then tend to decrease the concentrations of A_T and DIC. The overall effect is actually that A_T and DIC concentrations decrease when runoff and loads increase, because the salinity effect on the concentrations is larger than the river load effect. Interestingly, pH is only marginally affected compared to the REF simulation (Table 3).

Changing DIC loads without corresponding changes in A_T loads (or vice versa) is not very realistic considering that both DIC and A_T usually consist mainly of bicarbonate. In the model where DIC and A_T are independent state variables, it is however from a technical point of view not a problem changing just one of them. In theory, one could consider a change in just the DIC loads (model experiments #28–31, Table 2) as a result of changing only the CO_2 part of DIC (CO_2 is not a part of A_T), which could correspond to changes in the respiration of organic carbon in the catchments. Realistic or not, the point with such experiments is to highlight the strong control exerted by A_T and atmospheric pCO_2 on the background DIC concentration (and pH), so that changes in DIC land loads are almost completely compensated by air-sea CO_2 fluxes at least on annual and longer time-scales (Table 4 and Fig. S2, Supporting information), so that the DIC and pH levels are only very marginally modified (Table 3).

4.4.1. Northern versus southern catchments

One thing that is of particular interest in terms of e.g. A_T and pH change is the response to future gradients in precipitation change. It has been suggested that precipitation and runoff could increase in the boreal (northern) catchments, but in contrast decrease in the continental (southern) catchments (Graham, 2004). More recent runoff projections (Saraiva et al., 2019) rather indicate overall increases in runoff, but with the most pronounced effect in northern catchments and a comparatively small increase or no change in southern catchments.

Catchments in the boreal part of the Baltic Sea drainage basin are typically dominated by silicate minerals. Rivers entering the northernmost sub-basins (the Bothnian Sea and Bay, see Fig. 1) are as a consequence characterized by low A_T concentrations – approximately 230 μmol kg^{-1} on average (zero-salinity end-member, see Beldowski et al. (2010)). The southern, continental catchments are in contrast dominated by carbonate minerals, and rivers are characterized by high A_T concentrations (e.g. ~3200 μmol kg^{-1} in rivers entering the Gulf of Riga, see Beldowski et al. (2010)). Runoff to the Bornholm Basin and the Gotland Sea is a mixture of high-A_T water from continental rivers (mainly Polish and Lithuanian rivers) and comparatively low-A_T water from Swedish rivers, respectively. The runoff to the Gotland Sea is however dominated by the continental Wisła and Nemunas rivers (~80% of the total runoff to the Gotland Sea), and the runoff to the Bornholm Basin is dominated by the continental Odra river (~90% of the total runoff to the Bornholm Basin) (cf. Kuliński and Pempkowiak, 2011).

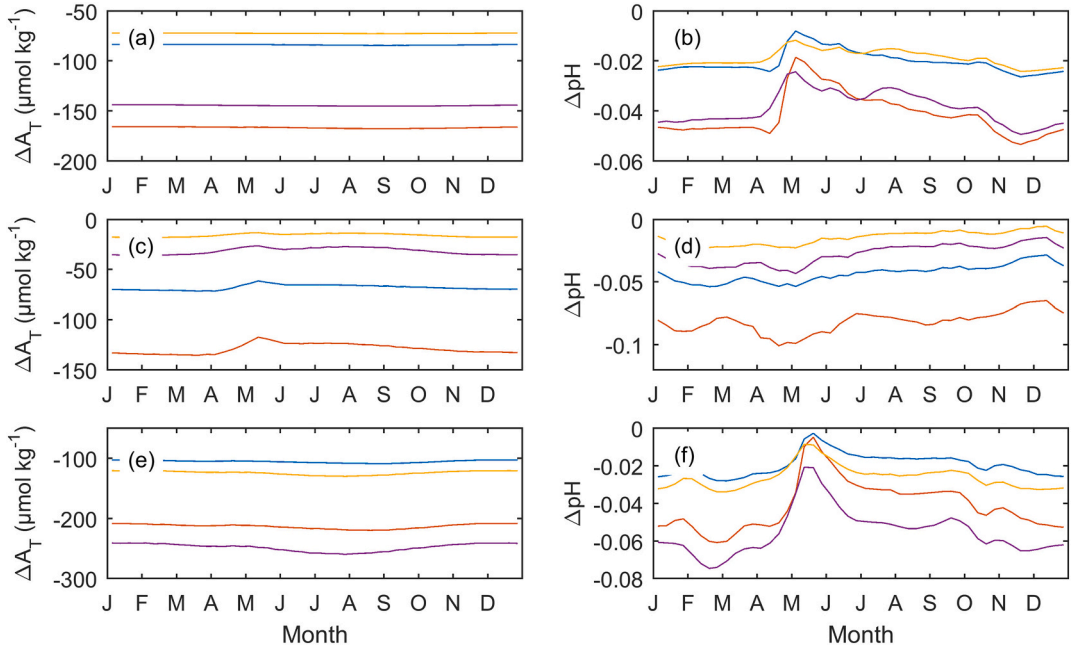

Fig. 5. A_T and pH change (ΔA_T and ΔpH respectively) in the Gotland Sea (a and b), the Bothnian Bay (c and d), and the Gulf of Riga (e and f) resulting from changes in runoff (and A_T and DIC loads) by ± 10% (blue lines) or ± 20% (red lines), or, changes only in riverine A_T and DIC concentrations by ± 10% (yellow lines) or ± 20% (purple lines) (see text in Section 4.4.1). (For interpretation of the references to color in this figure legend, the reader is referred to the web version of this article.)

The sensitivity to a development with increased precipitation in northern catchments and reduced precipitation in southern catchments is examined first by increasing the runoff and A_T and DIC loads in the Bothnian Sea and Bay by either 10 or 20%, and simultaneously decreasing the runoff and A_T and DIC loads to the Bornholm Basin, the Gotland Sea, and the Gulf of Riga by 10 and 20% (model experiments #32–33, Table 2). In these cases, the total land loads of A_T to the Baltic Sea decrease by approximately 6.3 and 13%, respectively. Similarly, the total land loads of DIC to the Baltic Sea decrease by 5.6 and 11% (see Table 2). Furthermore, the total runoff to the Bothnian Sea and Bay is on average 190 km^3 $year^{-1}$ in the REF simulation, whereas the total runoff to the Bornholm Basin, the Gotland Sea, and the Gulf of Riga is on average 144 km^3 $year^{-1}$. This means that in addition to the impact of changing A_T and DIC land loads, there is also a salinity effect because of the modified overall freshwater supply to the entire Baltic Sea. In order to separate the effects related to changes in loads and salinity, respectively, we did additional model runs where only the riverine A_T and DIC concentrations were changed by ± 10 or ± 20% (same sub-basins as before), but the runoff was not altered (model experiments #34–35, Table 2).

In Fig. 5, average seasonal changes in A_T and pH (ΔA_T and ΔpH) between the different experiments described above and the REF simulation, respectively, are presented for three sub-basins – the Gotland Sea, the Bothnian Bay, and the Gulf of Riga. In the Bothnian Bay, the largest reductions in both A_T and pH occur in the cases were runoff changes together with the A_T and DIC loads, illustrating the relatively strong influence of salinity on the carbonate system in this sub-basin (Fig. 5c and d). However, even in the cases where only the riverine concentrations (but not the runoff) changes (by 10 or 20%), both A_T and pH decrease in the Bothnian Bay in spite of the increased land loads. This illustrates the importance of water exchange between the Bothnian Sea, the Bothnian Bay, and the Gotland Sea. A_T decreases in the Gotland Sea by varying amounts in all four sensitivity experiments (Fig. 5a). In the Gotland Sea, the salinity effect is less pronounced than in the Bothnian Bay, although we do see a similar pattern – with a larger reduction in both A_T and pH in the cases where both runoff and loads change simultaneously (Fig. 5a and b). In the Gulf of Riga, the largest reductions in A_T and pH occur in the cases where A_T and DIC land loads are reduced by 20%, as expected (Fig. 5e and f). In contrast to the Bothnian Bay and the Gotland Sea, the A_T reduction in the Gulf of

Table 5
System-scale integrated A_T fluxes (Gmol $year^{-1}$) related to production and mineralization processes in the different nutrient load scenarios (REF, BSAP, HEL, and HIGH, see Sections 2.3–2.4) averaged over the last 100 years of the simulations.

Process	REF	BSAP	HEL	HIGH
Pelagic				
Nitrate assimilation	174.6	125.2	220.8	383.6
Ammonium assimilation	−85.2	−26.4	−155.1	−400.8
Ammonification	183.2	84.8	291.3	675.4
Nitrification	−223.0	−140.0	−310.8	−652.9
Denitrification	3.2	0.1	10.2	39.5
Phosphate assimilation	18.0	9.9	26.2	54.9
Phosphate release	−11.5	−5.1	−18.5	−43.6
Sulfate reduction	0.3	0.0	5.4	56.7
Sulfide oxidation	−3.5	−0.1	−35.2	−299.4
Total pelagic	56.0	48.5	34.1	−186.5
Benthic				
Ammonification	100.1	76.3	118.1	172.4
Nitrification	−198.6	−151.9	−227.8	−283.8
Denitrification	64.9	48.3	74.7	89.4
Phosphate release	−5.9	−4.5	−7.0	−10.4
Sulfate reduction	3.3	0.1	30.2	243.1
Total benthic	−36.2	−31.8	−11.9	210.7
Pelagic plus benthic				
Net N cycling	19.2	16.3	21.3	22.8
Net P cycling	0.6	0.4	0.6	0.9
Net S cycling	0.1	0.0	0.3	0.4
Total A_T sources minus sinks	19.8	16.7	22.2	24.2

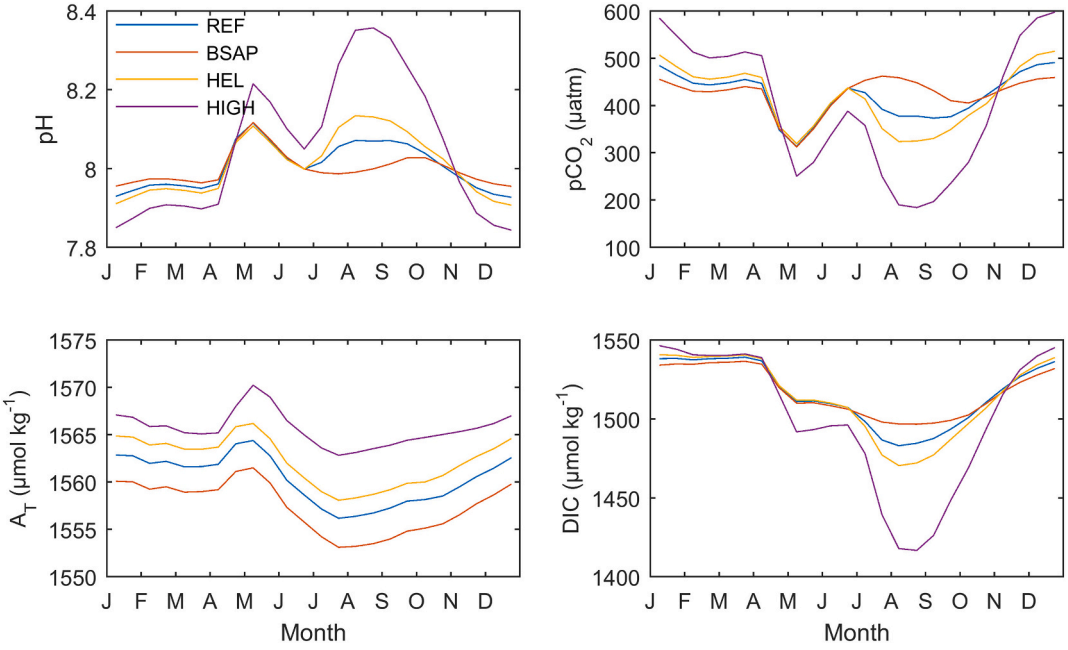

Fig. 6. Average seasonal development of pH, pCO_2, A_T, and DIC in Gotland Sea surface water in the REF (blue), BSAP (red), HEL (yellow), and HIGH (purple) simulations (see Sections 2.3–2.4). (For interpretation of the references to color in this figure legend, the reader is referred to the web version of this article.)

Riga is smaller in the case where both runoff and loads decrease compared to the case where only loads but not runoff decrease.

4.5. Internal production and consumption of A_T

A_T is produced and consumed because of primary production and mineralization processes. BALTSEM separates the external supplies of organic N and P, nitrate, ammonium, and phosphate, respectively, and computes their cycling (assimilation by autotrophs and remineralization in water column and sediments) and ultimate fates (burial, denitrification, export out of the system). The influence on A_T by these processes (see Appendix A3 for detailed descriptions) are computed as well. We furthermore include the A_T production and consumption associated with pelagic and benthic sulfate reduction during anaerobic mineralization as well as oxidation of sulfide at the pelagic oxycline.

The A_T sources and sinks related to the cycling on N, P, and S in the four different nutrient load scenarios, i.e., the REF simulation (see Section 2.3), and the BSAP, HEL, and HIGH simulations respectively (model experiments #17–19, Table 2) are presented in Table 5. In the BSAP experiment, S cycling has a very minor influence on A_T production/consumption in both sediments and water column, a result of the very favorable oxygen conditions in this simulation (Fig. S3, Supporting information). In the HIGH scenario, with extremely high N and P loads and oxygen deteriorated conditions, there is in contrast a very large A_T generation resulting from sulfate reduction in the sediments (Table 5). However, this A_T source is counteracted by A_T consumption through sulfide oxidation in the water column. The long-term net effect of pelagic and benthic S cycling is thus marginal on a system scale in all nutrient load scenarios, although the decadal trends are substantial in the HIGH scenario (Fig. S4d, Supporting information). As discussed by Gustafsson et al. (2019a, 2019b), there should be a net A_T production associated with permanent S burial in the form of e.g. pyrite. But, BALTSEM does not include iron which means the potential A_T generation by pyrite burial cannot be explicitly addressed.

Based on observations of nitrate and oxygen in the Baltic Sea over the last 50 years, it has been demonstrated that on a basin-scale, there is a negative correlation between the total nitrate pool and the volume of hypoxic water (Savchuk, 2018). This can be explained by enhanced nitrate losses by e.g. denitrification during oxygen deteriorated conditions (and vice versa). Denitrification is also a source for A_T (Table A2, Appendix A3), but a net source only if the removed nitrate was allochthonous by origin (e.g. Hu and Cai, 2011). Thus, even though the denitrification fluxes are very large in the HIGH scenario, most of this A_T source is balanced by other (A_T consuming) processes of the N cycling. We find that on a system scale, the net A_T production by N cycling (and overall) is similar in the different nutrient load scenarios (Table 5). Nevertheless, the HIGH scenario produces the highest A_T concentrations, whereas the BSAP scenario produces the lowest (Table 5).

Average seasonal developments of pH, pCO_2, A_T, and DIC in Gotland Sea surface water for the four nutrient load scenarios are indicated in Fig. 6. The large seasonal pH change is largely a result of CO_2 uptake/release and thus changes in DIC concentration. A_T varies less over the year and has a comparatively marginal influence on the seasonal pH dynamics. In addition to the highest A_T concentration, the HIGH scenario also produces the lowest DIC concentration (and vice versa for the BSAP scenario). This is a result of the comparatively high CO_2 uptake by autotrophs in the productive season – fueled by enhanced nutrient levels. The very high pCO_2 drawdown is partly but not completely compensated by the comparatively sluggish air-sea CO_2 fluxes, and this is the only one of the nutrient load scenarios where the Baltic Sea is a net sink for atmospheric CO_2 (Table 4). Of the nutrient load scenarios, the HIGH scenario produces by far the highest pH during the productive season, and also the highest annual mean pH. However, this scenario also produces the lowest pH in winter because of entrainment of CO_2-enriched sub-surface waters. The HIGH scenario thus produces the largest seasonal pH range, and, in terms of what organisms actually experience (rather than the long-term mean), the most acidified wintertime conditions of all nutrient load scenarios.

4.5.1. Theoretical impact on A_T by cycling of allochthonous N and P

In the results presented for the last hundred years of the different scenarios, the model has as already mentioned reached a quasi-steady

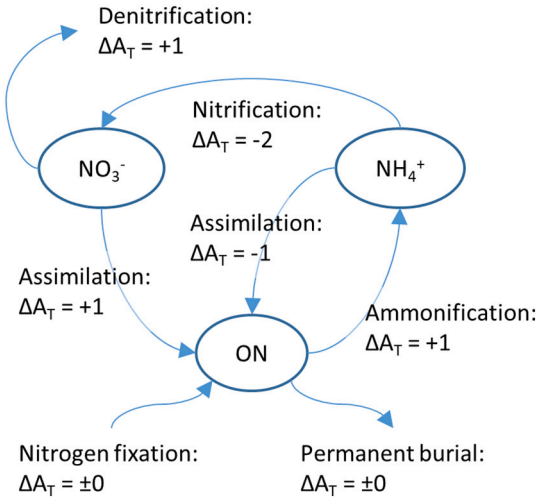

Fig. 7. A_T production and consumption related to N transformations (unit: mole A_T change per mole N change, see text in Section 4.5.1).

state (see Section 2.2) where external sources of e.g. nutrients are essentially in balance with loss terms. Externally supplied organic N and P can either be cycled and removed within the system or exported to the North Sea in case of more refractory dissolved organic N and P fractions. In the Baltic Sea and other systems with long residence times, the theoretical impact of nutrient cycling on A_T can be estimated by assuming that all of the inorganic nutrients supplied by terrestrial and atmospheric sources are removed within the system (ignoring exchange between the Baltic and North Seas), i.e., the external sources of degradable nutrients are balanced by internal sinks.

If the exchange between the Baltic and North Seas is ignored, N can be removed either by permanent burial or denitrification, whereas the only sink for P is burial. Regardless of pathways in the system and ultimate fate (i.e., burial or denitrification), removal of allochthonous nitrate produces A_T whereas removal of allochthonous ammonium on the other hand consumes A_T. Removal of allochthonous phosphate (by primary production followed by burial) produces A_T. Removal of allochthonous organic N and P has no net effect on A_T – this is also the case for cycling of N that was originally atmospheric N_2 fixed by cyanobacteria (see Wolf-Gladrow et al., 2007). The A_T sources and sinks related to N cycling are schematically illustrated in Fig. 7 (and described in detail in Table A2).

In order to understand the A_T generation coupled to nutrient cycling – with very large individual fluxes but only a comparatively small overall net effect (Table 5) – it is possible to assess an "upper limit" for A_T generation based on external loads of N and P. Under the assumption that external loads of inorganic N and P are balanced by equally large internal sinks, a theoretical internal A_T generation can be estimated from the magnitudes of external inorganic N and P loads. In Table 6, the external loads of ammonium, nitrate, and phosphate (converted from ktons year^{-1} to Gmol year^{-1}) according to the different scenarios are listed. The theoretical A_T generation is estimated by assuming that external sources of inorganic nutrients are balanced by equally large internal sinks so that the nitrate and phosphate supplies correspond to A_T sources and the ammonium supply corresponds to an A_T sink (1:1 molar ratios). These theoretical fluxes are indeed very similar to the net fluxes from N and P cycling presented in Table 4.

It is worth noting that the external supplies of nutrients (Table 6) are very small compared to the fluxes associated with primary production and respiration processes (Table 5), illustrating how nutrients can be recycled many times before they are permanently removed from the loop (cf. Gustafsson et al., 2012). In addition, the external loads are typically very small compared to the nutrient reservoirs in the system (Gustafsson et al., 2017).

4.6. Ocean water properties

Oceanic A_T and DIC concentrations are usually assumed to be stable over time, although in particular in the case of DIC, latitude dependent (e.g. Sarmiento and Gruber, 2006). Seasonal variations of mainly DIC result from soft-tissue production (CO_2 assimilation by autotrophs), whereas both A_T and DIC are affected by $CaCO_3$ formation ($Ca^{2+} + 2HCO_3^- \rightarrow CaCO_3 + H_2CO_3$). Spring/summer blooms of coccolithophores are occasionally observed in the Baltic Sea entrance area (the Kattegat, see Fig. 1), whereas in the North Sea outside the Baltic Sea entrance area, blooms of the coccolithophore *Emiliania huxleyi* have been frequently reported (Holligan et al., 1993). For that reason, seasonal variations of A_T and DIC at the ocean boundary decoupled from the linear salinity relationships described in Section 2.3 can be expected. Furthermore, oceanic A_T can change over time either as a result of changes in weathering of continental rocks, or, as discussed by Boudreau et al. (2018), large-scale changes in calcification rates (i.e., $CaCO_3$ production). This means that the experiments with changing DIC and A_T concentrations at the ocean boundary (model experiments #20–23, Table 2) – although speculative – give an indication of the pH sensitivity of Baltic Sea waters to potential real future changes of ocean water properties.

4.7. Response times

Response times of quantities changing exponentially over time can be estimated by means of "decay rates" using an e-folding time-scale, i.e., the time it takes for a quantity to shrink to e.g. 1/e (or ~ 37%) or 1/e^3 (or ~ 5%) of its initial value. Here we apply this concept on carbonate system parameters based on the response time experiments described in Section 2.5.

Fig. 8 shows the development of DIC, pH, and pCO_2 in the first year (i.e., model year 0) after the abrupt changes in atmospheric pCO_2 took place (model experiments #36–37, Table 7). Air-sea CO_2 exchange is often described as sluggish (at least compared to exchange of other gasses that do not react with water), but, the e-folding time-scale of surface water pCO_2, pH, and DIC is approximately 1 month (Table 7). A_T is not affected by pCO_2 change since the model does not include $CaCO_3$ formation/dissolution (see Section 4.2) – A_T is for that reason not included in Fig. 8. In this particular year, there was no deep water inflow in the model, which means that carbonate system parameters in the isolated deep waters have not yet responded to the pCO_2 change.

In the experiments with abrupt changes in either runoff, A_T and DIC

Table 6
Theoretical A_T generation (Gmol year^{-1}) by cycling of externally supplied inorganic N (=nitrate supply − ammonium supply) and P (=phosphate supply) respectively (see text in Section 4.5.1).

Model run	Case	Nitrate supply (Gmol year^{-1})	Ammonium supply (Gmol year^{-1})	Phosphate supply (Gmol year^{-1})	Theoretical A_T generation by N cycling (Gmol year^{-1})	Theoretical A_T generation by P cycling (Gmol year^{-1})
#1	REF	31.8	11.6	0.5	20.3	0.5
#17	BSAP	27.9	10.1	0.3	17.8	0.3
#18	HEL	37.0	14.1	0.5	22.9	0.5
#19	HIGH	46.5	20.4	1.1	26.1	1.1

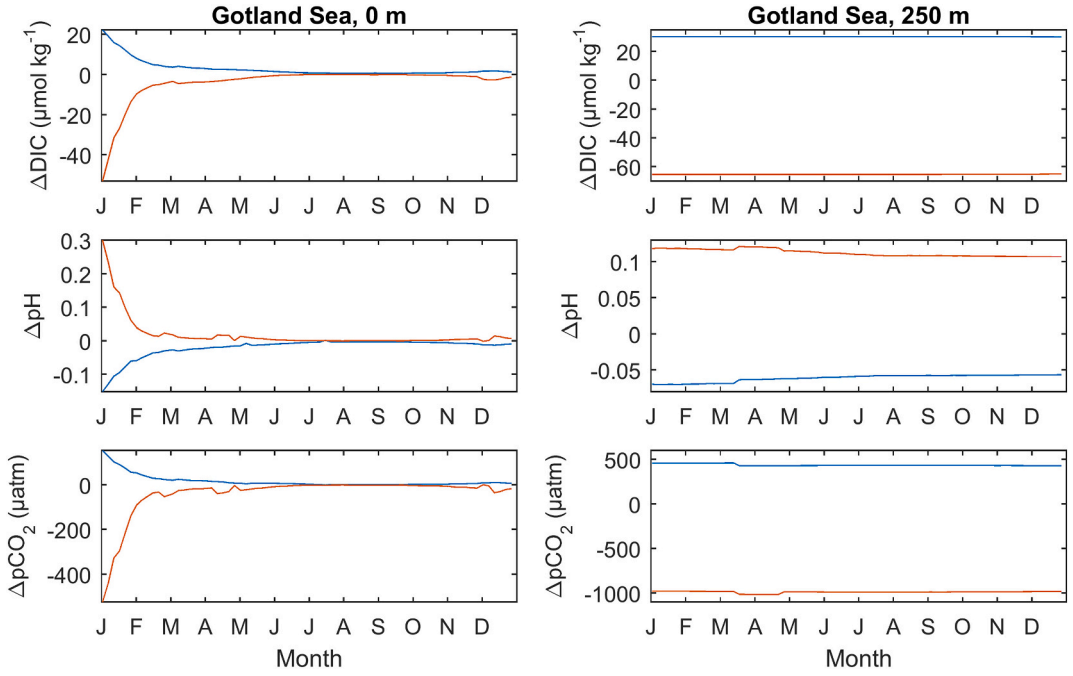

Fig. 8. Response of DIC, pH, and pCO_2 in the Gotland Sea to sudden changes in atmospheric pCO_2: lines indicate differences (Δ) between model run #36 and #2 (blue) and model run #37 and #4 (red) (see further Tables 2 and 7 and also text in Section 4.7). (For interpretation of the references to color in this figure legend, the reader is referred to the web version of this article.)

Table 7
Response times (e-folding time-scale) of carbonate system parameters to instantaneous changes in forcing compared to the REF simulation (see Sections 2.5 and 4.7).

Model run	Factor addressed	Instantaneous change year 0	e-Folding time-scale
#36	Atmospheric pCO_2	REF pCO_2 to pre-industrial pCO_2	~1 month
#37	Atmospheric pCO_2	REF pCO_2 to pCO_2 according to RCP 8.5	~1 month
#38	River runoff	Runoff increased by 10%	~30 years
#39	River runoff	Runoff increased by 20%	~30 years
#40	A_T/DIC land loads	A_T/DIC land loads increased by 10%	~30 years
#41	A_T/DIC land loads	A_T/DIC land loads increased by 20%	~30 years
#42	N/P loads (land + atm.)	REF N/P loads to BSAP N/P loads	Not applicable
#43	N/P loads (land + atm.)	REF N/P loads to HIGH N/P loads	Not applicable
#44	Ocean A_T/DIC	Ocean A_T/DIC increased by 10%	~30 years
#45	Ocean A_T/DIC	Ocean A_T/DIC increased by 20%	~30 years

land loads, or oceanic A_T and DIC concentrations (exemplified by changes in A_T and DIC land loads in Fig. 9), the e-folding time-scales are consistently found to be approximately 30 years (model experiments #38–41 and #44–45, Table 7). According to these experiments it will furthermore take approximately 90 years to reduce the initial imbalances to 5%. This is what would be expected, considering that the response times in these cases are closely related to the overall residence times of water and salt in the system (~35 years; Stigebrandt and Gustafsson, 2003). pCO_2 is not included in Fig. 9, the reason being the comparatively fast response of pCO_2 as described above.

Nutrient cycling is coupled to the overall water exchange of the Baltic Sea. However, because of different internal biogeochemical processes related to e.g. oxygen conditions, residence times for N and P are quite different from one another – approximately 10 years for N and 50 years for P (Gustafsson et al., 2017). Relations between nutrient loads, productivity patterns, and oxygen conditions are complex and non-linear, phenomena that are also reflected in the long-term response of carbonate system parameters to sudden changes in nutrient loads (model experiments #42–43, Table 7). Compared to the experiments described above, it is less straightforward to determine exponential changes of carbonate system parameters over time, although the response times are similar to those found in the experiments more directly coupled to water exchange (Fig. 10).

4.8. Future outlook

The main objective of the present study has been to single out key processes that influence carbonate system parameters, quantify their potential impact, and compare their relative importance for e.g. pH change. In order not to weigh down the manuscript, we did not include coupled climate change/land-use change/global mean sea level change scenarios – the intention is to investigate such future projections in a follow-up study, including also the potential impact of pH change on biota.

5. Conclusions

Based on our sensitivity experiments we identify several processes that could, if not increase pH, at least to some degree mitigate the ongoing CO_2-induced ocean acidification. These processes are: reduced

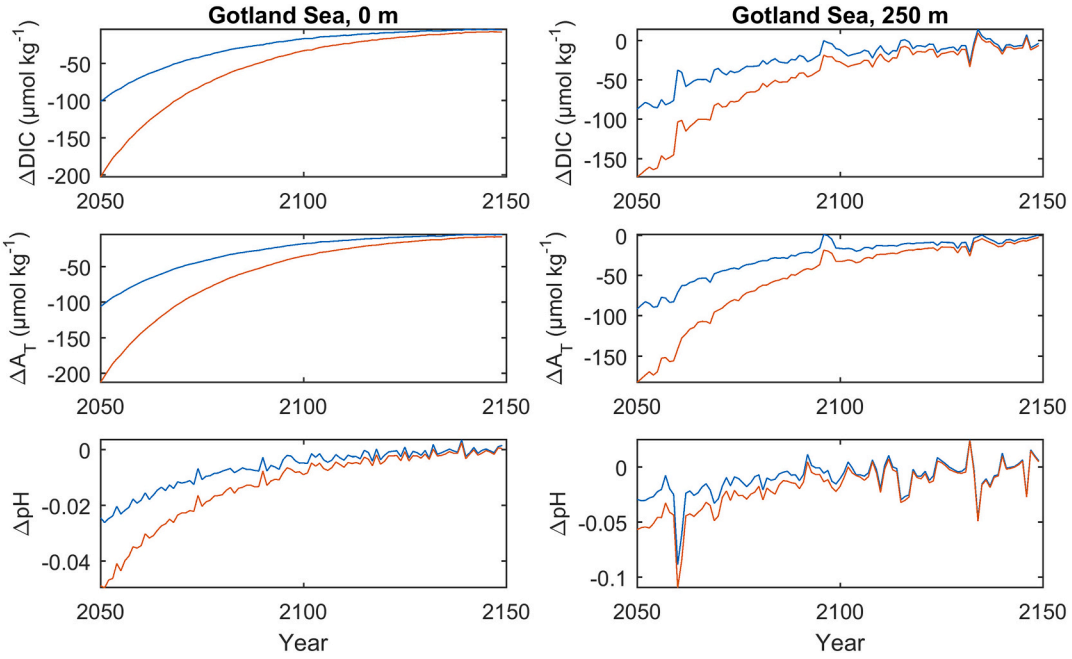

Fig. 9. Response of DIC, A_T, and pH in the Gotland Sea to sudden changes in land loads of A_T and DIC: lines indicate differences (Δ) between annual mean values from model run #40 and #15 (blue) and model run #41 and #16 (red) (see further Tables 2 and 7 and also text in Section 4.7). (For interpretation of the references to color in this figure legend, the reader is referred to the web version of this article.)

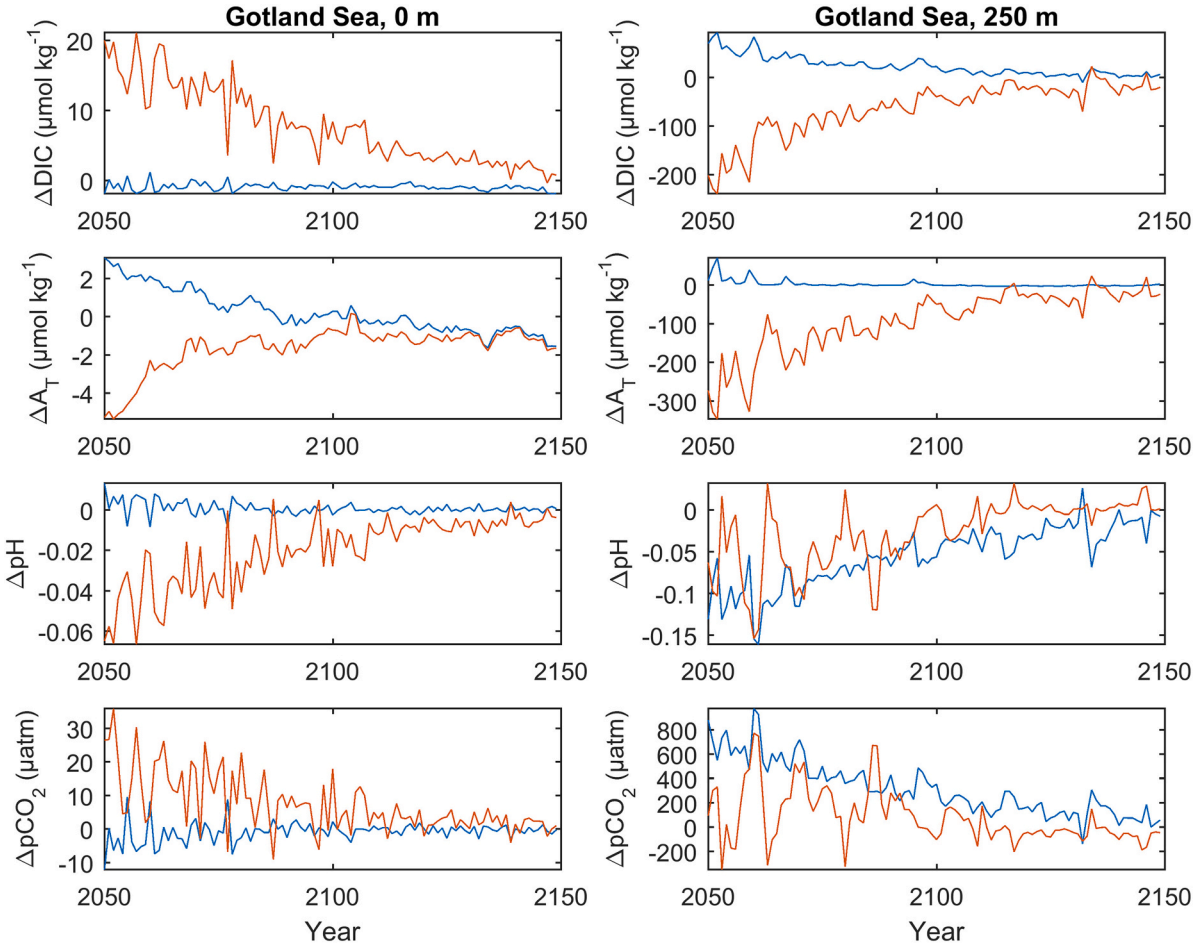

Fig. 10. Response of DIC, A_T, pH, and pCO_2 in the Gotland Sea to sudden changes in nutrient loads: lines indicate differences (Δ) between annual mean values from model run #42 and #17 (blue) and model run #43 and #19 (red) (see further Tables 2 and 7 and also text in Section 4.7). (For interpretation of the references to color in this figure legend, the reader is referred to the web version of this article.)

runoff (salinity effect), increased riverine and/or ocean water A_T concentrations (buffering effect), or increased nutrient loads and productivity (CO_2 assimilation and internal A_T generation effects). Consequently, future acidification could be more severe than from the atmospheric CO_2 effect alone because of increased runoff (desalination), reduced riverine and/or oceanic A_T, or reduced nutrient loads and productivity (oligotrophication). It is however important to note that although summertime and also the annual mean surface water pH are enhanced in a eutrophied, oxygen deteriorated Baltic Sea, the wintertime pH – which is also the annual pH minimum – is actually lower in this scenario than in the ones with lower nutrient loads and better oxygen conditions. Thus, it is in the BSAP scenario with comparatively low nutrient loads and favorable oxygen conditions that we observe the smallest wintertime pH reduction.

Future climate change projections indicate increased runoff to the Baltic Sea, in particular to northern catchments with low-A_T river water. In addition to the A_T and pH reduction related to desalination, a further reduction can be expected by changing the proportions of river water coming from silicate dominated and limestone dominated catchments, respectively.

We can furthermore quantify the potential pH change coupled to the different model forcing factors described above. In most cases, pH changes are in a range of approximately ± 0.05 pH units, but strongly dependent on the magnitude of the "disturbance". In the cases with modified atmospheric pCO_2 we find the largest effects on pH. It seems highly unlikely that the pH reduction following more than a doubling of the atmospheric pCO_2 (the RCP 8.5 case) could be counteracted by any of the other pH influencing processes described in this study.

Declaration of competing interest

The authors declare that they have no known competing financial interests or personal relationships that could have appeared to influence the work reported in this paper.

Acknowledgements

This study was supported by the OMAI project funded by the Nordic Council of Ministers (Grant #190009) and BONUS COCOA funded by Formas and the European Commission. The Baltic Nest Institute is supported by The Swedish Agency for Marine and Water Management through their grant 1:11 - Measures for marine and water environment. Erik Smedberg is acknowledged for contributions to the artwork.

Appendix A

A1. Model description

All state variables (pelagic and benthic) that are included in BALTSEM are indicated in Table A1. A schematic illustration of processes included in the cycling of nutrients and carbon is presented in Fig. A1.

Table A1
Pelagic and benthic state variables in BALTSEM.

State variable	Description	Unit
Pelagic		
S	Salinity	–
T	Temperature	°C
O_2	Dissolved oxygen	g O_2 m^{-3}
NH_4	Total ammonia (NH_3 + NH_4^+)	mg N m^{-3}
NO_3	Oxidized N (NO_3^- + NO_2^-)	mg N m^{-3}
PO_4	Phosphate (H_3PO_4 + $H_2PO_4^-$ + $HPO_4^=$ + PO_4^{3-})	mg P m^{-3}
Si_T	Dissolved silica ($Si(OH)_4$ + $SiO(OH)_3^-$)	mg Si m^{-3}
D_N	Detrital N	mg N m^{-3}
D_P	Detrital P	mg P m^{-3}
D_{Si}	Detrital Si, biogenic Si	mg Si m^{-3}
D_{CM}	Detrital C (autochthonous)	mg C m^{-3}
D_{CT}	Detrital C (allochthonous)	mg C m^{-3}
A_1	Autotroph group 1, cyanobacteria	mg N m^{-3}
A_2	Autotroph group 2, diatoms	mg N m^{-3}
A_3	Autotroph group 3, summer species	mg N m^{-3}
Z_H	Heterotroph community	mg N m^{-3}
DIC	Dissolved inorganic carbon	µmol kg^{-1}
A_T	Total alkalinity	µmol kg^{-1}
H_2S	Total hydrogen sulfide (HS^- + H_2S)	µmol kg^{-1}
DONL	Labile dissolved organic N	mg N m^{-3}
DONR	Refractory dissolved organic N	mg N m^{-3}
DOPL	Labile dissolved organic P	mg P m^{-3}
DOPR	Refractory dissolved organic P	mg P m^{-3}
$DOCL_M$	Labile dissolved organic C (autochthonous)	mg C m^{-3}
$DOCR_M$	Refractory dissolved organic C (autochthonous)	mg C m^{-3}
$DOCL_T$	Labile dissolved organic C (allochthonous)	mg C m^{-3}
$DOCR_T$	Refractory dissolved organic C (allochthonous)	mg C m^{-3}
Benthic		
B_N	Benthic organic N	mg N m^{-2}
B_P	Benthic organic P	mg P m^{-2}
B_{Si}	Benthic biogenic Si	mg Si m^{-2}
B_{CM}	Benthic organic C (autochthonous)	mg C m^{-2}
B_{CT}	Benthic organic C (allochthonous)	mg C m^{-2}

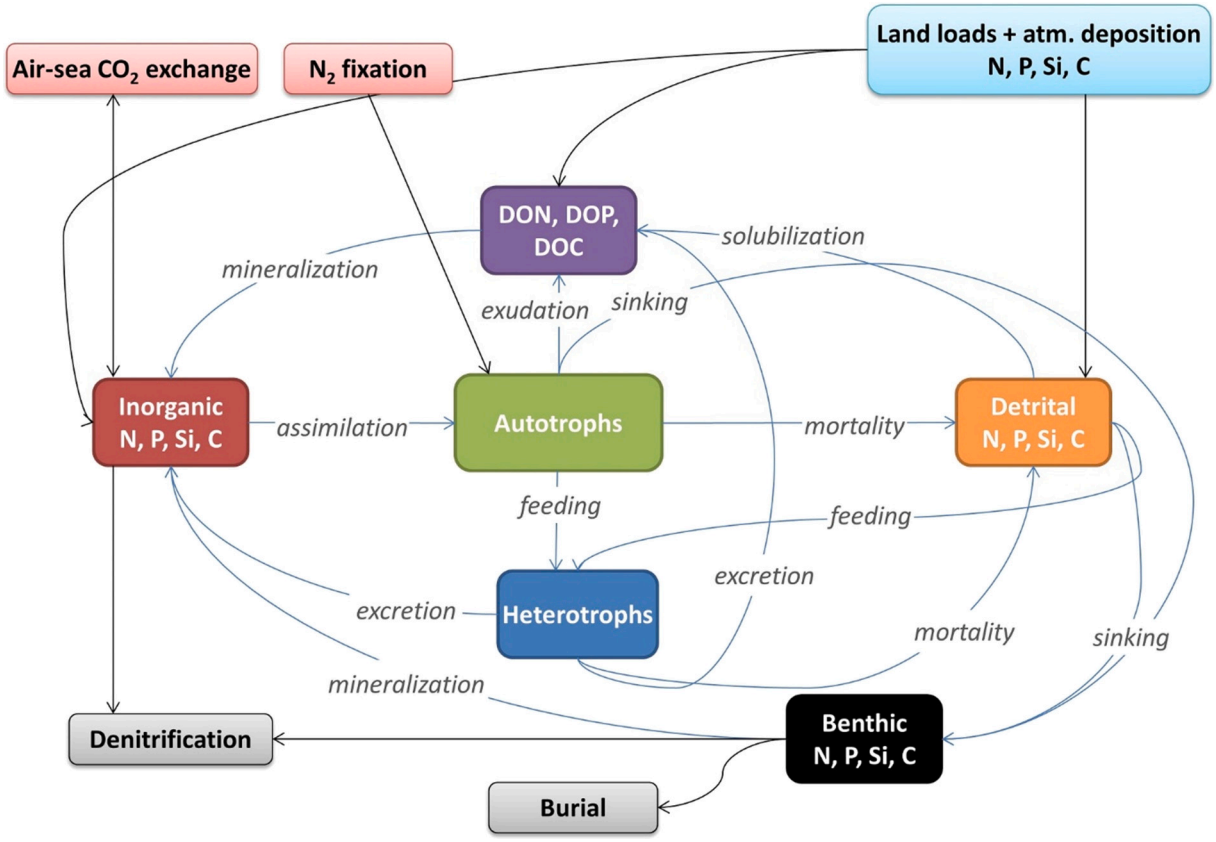

Fig. A1. Schematic illustration of biogeochemical processes included in BALTSEM.

A2. The marine carbonate system parameters

A short description of the four carbonate system DIC, A_T, pH, and pCO_2 follows below. Detailed descriptions are available in e.g. Dickson et al. (2007).

DIC

The concentration of DIC in seawater is defined as

$$DIC = [CO_2^*] + [HCO_3^-] + [CO_3^=] \quad \text{(A1)}$$

where

$$[CO_2^*] = [CO_2] + [H_2CO_3] \quad \text{(A2)}$$

A_T

The A_T definition used in BALTSEM is based on Dickson (1981) but also includes organic alkalinity based on Kuliński et al. (2014) and Ulfsbo et al. (2015):

$$A_T = [HCO_3^-] + 2[CO_3^=] + [B(OH)_4^-] + [OH^-] + [HPO_4^=] + 2[PO_4^{3-}] + [SiO(OH)_3^-] + [NH_3] + [HS^-] - [H^+] - [HF] - [H_3PO_4] + organic\ alkalinity \quad \text{(A3)}$$

$[H^+]$ is here the sum of "free" hydrogen ion and hydrogen sulfate ion concentrations:

$$[H^+] = [H^+]_F + [HSO_4^-] \quad \text{(A4)}$$

pH

The $[H^+]$ concentration is expressed by pH (using the total pH scale, i.e., $[H^+]$ according to Eq. (A4))

$$pH = -\log[H^+] \quad \text{(A5)}$$

pCO_2

The "effective" partial pressure (or fugacity) of CO_2 is not exactly the same as its mechanical partial pressure (although very nearly so) since it accounts for the fact that CO_2 is not an ideal gas. In this study the effective partial pressure is denoted by pCO_2 and defined as

$$pCO_2 = \frac{[CO_2^*]}{k_0} \quad \text{(A6)}$$

where k_0 is the solubility constant (Weiss, 1974).

A3. Internal sources and sinks of A_T

Using the electroneutrality compensation principle for nutrient assimilation as described by Wolf-Gladrow et al. (2007), assimilation of 1 mole NO_3^- (or NO_2^-) increases A_T by 1 mol (reaction R1, Table A2), assimilation of 1 mole NH_4^+ decreases A_T by 1 mol (R2), fixation of atmospheric N_2 has no impact on A_T. Assimilation of 1 mol of phosphate (regardless of form: H_3PO_4, $H_2PO_4^-$, $HPO_4^=$, or PO_4^{3-}) increases A_T by 1 mol (R1–R2). Ammonification increases A_T by 1 mol per 1 mol of NH_4^+ production, nitrification consumes 2 mol of A_T per 1 mol of oxidized ammonium (R4), whereas denitrification produces 1 mol of A_T per 1 mol of removed NO_3^- (R5 and R6). Sulfate reduction generates 2 mol of A_T per 1 mol of reduced sulfate (R7), whereas sulfide oxidation consumes 2 mol of A_T per 1 mol of oxidized sulfide (R8). A_T is further influenced by cycling of iron and manganese, but these processes are not included in BALTSEM (cf. Gustafsson et al., 2019a, 2019b).

The production and consumption of A_T coupled to biogeochemical processes that are included in BALTSEM are summarized in Table A2. Organic material (OM) is here defined as $(CH_2O)_a(NH_3)_b(H_3PO_4)_c$, where a:b:c denotes the molar C:N:P ratios.

Table A2
Cycling of N, P, and S, and the related generation/consumption of A_T (ΔA_T) due to primary production and mineralization processes included in BALTSEM.

	Process	Reaction	ΔA_T
R1	NO_3^- uptake	$aCO_2 + bNO_3^- + cHPO_4^{2-} + (b + 2c)H^+ + (a + b)H_2O \longrightarrow OM + (a + 2b)O_2$	b + c
R2	NH_4^+ uptake	$aCO_2 + bNH_4^+ + cHPO_4^{2-} + bOH^- + 2cH^+ + aH_2O \longrightarrow OM + aO_2 + bH_2O$	−b + c
R3	Ammonification	$OM + aO_2 + bH_2O \rightarrow aHCO_3^- + bNH_4^+ + bOH^- + cHPO_4^{2-} + 2cH^+$	b − c
R4	Nitrification	$2O_2 + NH_4^+ + 2HCO_3^- \longrightarrow NO_3^- + 2CO_2 + 3H_2O$	−2
R5	Heterotrophic denitrification	$OM + \frac{4a}{5}NO_3^- + bH_2O \longrightarrow \frac{a}{5}CO_2 + \frac{4a}{5}HCO_3^- + \frac{3a}{5}H_2O + \frac{2a}{5}N_2 + bNH_4^+ + cHPO_4^{2-} + bOH^- + 2cH^+$	0.8a + b − c
R6	Chemolithoautotrophic denitrification	$2NO_3^- + 5H_2S + 2H^+ \longrightarrow N_2 + 5S + 6H_2O$	2
R7	Sulfate reduction	$OM + \frac{a}{2}SO_4^= + bH_2O \longrightarrow aHCO_3^- + \frac{a}{2}H_2S + bNH_4^+ + cHPO_4^{2-} + bOH^- + 2cH^+$	a + b − c
R8	Sulfide oxidation	$2O_2 + H_2S + 2HCO_3^- \longrightarrow SO_4^= + 2CO_2 + 2H_2O$	−2

Appendix B. Supplementary data

Supplementary data to this article can be found online at https://doi.org/10.1016/j.jmarsys.2020.103397.

References

Beldowski, J., Löffler, A., Schneider, B., Joensuu, L., 2010. Distribution and biogeochemical control of total CO_2 and total alkalinity in the Baltic Sea. J. Mar. Syst. 81, 252–259. https://doi.org/10.1016/j.jmarsys.2009.12.020.

Boudreau, B.P., Middelburg, J.J., Luo, Y., 2018. The role of calcification in carbonate compensation. Nat. Geosci. 11, 894. https://doi.org/10.1038/s41561-018-0259-5.

Cai, W.-J., Hu, X., Huang, W.-J., Murrell, M.C., Lehrter, J.C., Lohrenz, S.E., Chou, W.-C., Zhai, W., Hollibaugh, J.T., Wang, Y., Zhao, P., Guo, X., Gundersen, K., Dai, M., Gong, G.-C., 2011. Acidification of subsurface coastal waters enhanced by eutrophication. Nat. Geosci. 4, 766–770. https://doi.org/10.1038/ngeo1297.

Carstensen, J., Duarte, C.M., 2019. Drivers of pH variability in coastal ecosystems. Environ. Sci. Technol. 53, 4020–4029. https://doi.org/10.1021/acs.est.8b03655.

Claremar, B., Rutgersson, A., 2017. 20th Century Deposition From Baltic Sea Ship Traffic (Version 1). Data set. Environment Climate Data Sweden (ECDS)https://doi.org/10.5879/ECDS/2017-10-10.2/1.

Dickson, A.G., 1981. An exact definition of total alkalinity and a procedure for the estimation of alkalinity and total inorganic carbon from titration data. Deep Sea Res. A Oceanogr. Res. Pap. 28, 609–623. https://doi.org/10.1016/0198-0149(81)90121-7.

Guide to best practices for ocean CO_2 measurements. In: Dickson, A.G., Sabine, C.L., Christian, J.R. (Eds.), PICES Special Publication 3, (191 pp).

Doney, S.C., Fabry, V.J., Feely, R.A., Kleypas, J.A., 2009. Ocean acidification: the other CO_2 problem. Annu. Rev. Mar. Sci. 1, 169–192. https://doi.org/10.1146/annurev.marine.010908.163834.

Ehrnsten, E., Norkko, A., Müller-Karulis, B., Gustafsson, E., Gustafsson, B.G., 2020. The meagre future of benthic fauna in a coastal sea – benthic responses to recovery from eutrophication under climate change. Glob. Chang. Biol. 26 (4), 2235–2250.

Eilola, K., Gustafsson, B.G., Kuznetsov, I., Meier, H.E.M., Neumann, T., Savchuk, O.P., 2011. Evaluation of biogeochemical cycles in an ensemble of three state-of-the-art numerical models of the Baltic Sea. J. Mar. Syst. 88, 267–284. https://doi.org/10.1016/j.jmarsys.2011.05.004.

Feely, R.A., Sabine, C.L., Lee, K., Berelson, W., Kleypas, J., Fabry, V.J., Millero, F.J., 2004. Impact of anthropogenic CO_2 on the $CaCO_3$ system in the oceans. Science 305, 362–366. https://doi.org/10.1126/science.1097329.

Fonselius, S., Valderrama, J., 2003. One hundred years of hydrographic measurements in the Baltic Sea. In: Journal of Sea Research, Proceedings of the 22nd Conference of the Baltic Oceanographers (CBO), Stockholm 2001, vol. 49. pp. 229–241. https://doi.org/10.1016/S1385-1101(03)00035-2.

Fransner, F., Gustafsson, E., Tedesco, L., Vichi, M., Hordoir, R., Roquet, F., Spilling, K., Kuznetsov, I., Eilola, K., Mörth, C.-M., Humborg, C., Nycander, J., 2018. Non-Redfieldian dynamics explain seasonal pCO_2 drawdown in the Gulf of Bothnia. J. Geophys. Res. Oceans 123, 166–188. https://doi.org/10.1002/2017JC013019.

Graham, L.P., 2004. Climate change effects on river flow to the Baltic Sea. AMBIO 33, 235–241. https://doi.org/10.1579/0044-7447-33.4.235.

Gustafsson, B.G., 2000. Time-dependent modeling of the Baltic entrance area. 1. Quantification of circulation and residence times in the Kattegat and the straits of the Baltic sill. Estuaries 23, 231–252. https://doi.org/10.2307/1352830.

Gustafsson, B.G., 2003. A Time-dependent Coupled-basin Model of the Baltic Sea, C47. Earth Sciences Centre, University of Gothenburg, Gothenburg.

Gustafsson, E., 2013. Modelling the marine CO_2 system in BALTSEM. In: BNI Technical Report No. 9.

Gustafsson, B.G., Stigebrandt, A., 2007. Dynamics of nutrients and oxygen/hydrogen sulfide in the Baltic Sea deep water. J. Geophys. Res. 112, G02023. https://doi.org/10.1029/2006JG000304.

Gustafsson, B.G., Schenk, F., Blenckner, T., Eilola, K., Meier, H.E.M., Müller-Karulis, B., Neumann, T., Ruoho-Airola, T., Savchuk, O.P., Zorita, E., 2012. Reconstructing the development of Baltic Sea eutrophication 1850–2006. AMBIO 41, 534–548. https://doi.org/10.1007/s13280-012-0318-x.

Gustafsson, E., Wällstedt, T., Humborg, C., Mörth, C.-M., Gustafsson, B.G., 2014. External total alkalinity loads versus internal generation: the influence of nonriverine alkalinity sources in the Baltic Sea. Glob. Biogeochem. Cycles 28, 2014GB004888. https://doi.org/10.1002/2014GB004888.

Gustafsson, E., Omstedt, A., Gustafsson, B.G., 2015. The air-water CO_2 exchange of a coastal sea—a sensitivity study on factors that influence the absorption and outgassing of CO_2 in the Baltic Sea. J. Geophys. Res. Oceans 120, 5342–5357. https://doi.org/10.1002/2015JC010832.

Gustafsson, E., Savchuk, O.P., Gustafsson, B.G., Müller-Karulis, B., 2017. Key processes in the coupled carbon, nitrogen, and phosphorus cycling of the Baltic Sea. Biogeochemistry 134, 301–317. https://doi.org/10.1007/s10533-017-0361-6.

Gustafsson, E., Hagens, M., Sun, X., Reed, D.C., Humborg, C., Slomp, C.P., Gustafsson, B.G., 2019a. Sedimentary alkalinity generation and long-term alkalinity development in the Baltic Sea. Biogeosciences 16, 437–456. https://doi.org/10.5194/bg-16-437-2019.

Gustafsson, E., Hagens, M., Sun, X., Reed, D.C., Humborg, C., Slomp, C.P., Gustafsson, B.G., 2019b. Corrigendum: sedimentary alkalinity generation and long-term alkalinity development in the Baltic Sea. Biogeosciences 16, 437–456. https://doi.org/10.5194/bg-16-437-2019.

HELCOM, 2013. HELCOM Copenhagen Ministerial Declaration. HELCOM Ministerial Meeting, Copenhagen October 3, 2013. Available at. http://helcom.fi.

HELCOM, 2015. Updated fifth Baltic Sea pollution load compilation (PLC-5.5). In: Baltic Sea Environment Proceedings No. 145, Available at. http://helcom.fi.

HELCOM, 2018. Inputs of nutrients (nitrogen and phosphorus) to the sub-basins of the Baltic Sea (2016). In: HELCOM Core Indicator Report, Available at. http://helcom.fi.

Holligan, P.M., Groom, S.B., Harbour, D.S., 1993. What controls the distribution of the coccolithophore, Emiliania huxleyi, in the North Sea? Fish. Oceanogr. 2, 175–183. https://doi.org/10.1111/j.1365-2419.1993.tb00133.x.

Hu, X., Cai, W.-J., 2011. An assessment of ocean margin anaerobic processes on oceanic alkalinity budget. Glob. Biogeochem. Cycles 25, GB3003. https://doi.org/10.1029/2010GB003859.

Kreus, M., Schartau, M., Engel, A., Nausch, M., Voss, M., 2015. Variations in the elemental ratio of organic matter in the central Baltic Sea: part I—linking primary production to remineralization. Cont. Shelf Res. 100, 25–45. https://doi.org/10.1016/j.csr.2014.06.015.

Krumins, V., Gehlen, M., Arndt, S., Van Cappellen, P., Regnier, P., 2013. Dissolved inorganic carbon and alkalinity fluxes from coastal marine sediments: model estimates for different shelf environments and sensitivity to global change. Biogeosciences 10, 371–398. https://doi.org/10.5194/bg-10-371-2013.

Kuliński, K., Pempkowiak, J., 2011. The carbon budget of the Baltic Sea. Biogeosciences 8, 3219–3230. https://doi.org/10.5194/bg-8-3219-2011.

Kuliński, K., Schneider, B., Hammer, K., Machulik, U., Schulz-Bull, D., 2014. The influence of dissolved organic matter on the acid–base system of the Baltic Sea. J. Mar. Syst. 132, 106–115. https://doi.org/10.1016/j.jmarsys.2014.01.011.

Leppäranta, M., Myrberg, K., 2009. Physical Oceanography of the Baltic Sea. Springer-Praxis, Heidelberg, Germany (378p).

Meier, H.E.M., Edman, M.K., Eilola, K.J., Placke, M., Neumann, T., Andersson, H.C., Brunnabend, S.-E., Dieterich, C., Frauen, C., Friedland, R., Gröger, M., Gustafsson, B.G., Gustafsson, E., Isaev, A., Kniebusch, M., Kuznetsov, I., Müller-Karulis, B., Omstedt, A., Ryabchenko, V., Saraiva, S., Savchuk, O.P., 2018. Assessment of eutrophication abatement scenarios for the Baltic Sea by multi-model ensemble simulations. Front. Mar. Sci. 5. https://doi.org/10.3389/fmars.2018.00440.

Mohrholz, V., 2018. Major baltic inflow statistics – revised. Front. Mar. Sci. 5. https://doi.org/10.3389/fmars.2018.00384.

Müller, J.D., Schneider, B., Rehder, G., 2016. Long-term alkalinity trends in the Baltic Sea and their implications for CO_2-induced acidification. Limnol. Oceanogr. 61 (6), 1984–2002. https://doi.org/10.1002/lno.10349.

Murray, C.J., Müller-Karulis, B., Carstensen, J., Conley, D.J., Gustafsson, B.G., Andersen, J.H., 2019. Past, present and future eutrophication status of the Baltic Sea. Front. Mar. Sci. 6. https://doi.org/10.3389/fmars.2019.00002.

Omstedt, A., Edman, M., Claremar, Bj., Frodin, P., Gustafsson, E., Humborg, C., Hägg, H., Mörth, M., Rutgersson, A., Schurgers, G., Smith, B., Wällstedt, T., Yurova, A., 2012. Future changes in the Baltic Sea acid–base (pH) and oxygen balances. Tellus 64B. https://doi.org/10.3402/tellusb.v64i0.19586.

Saraiva, S., Meier, H.E.M., Andersson, H., Höglund, A., Dieterich, C., Gröger, M., Hordoir, R., Eilola, K., 2019. Baltic Sea ecosystem response to various nutrient load scenarios in present and future climates. Clim. Dyn. 52, 3369–3387. https://doi.org/10.1007/s00382-018-4330-0.

Sarmiento, J.L., Gruber, N., 2006. Ocean Biogeochemical Dynamics. Princeton University Press, Princeton and Oxford (503 pp).

Savchuk, O.P., 2002. Nutrient biogeochemical cycles in the Gulf of Riga: scaling up field studies with a mathematical model. J. Mar. Syst. 32, 253–280. https://doi.org/10.1016/S0924-7963(02)00039-8.

Savchuk, O.P., 2018. Large-scale nutrient dynamics in the Baltic Sea, 1970–2016. Front. Mar. Sci. 5. https://doi.org/10.3389/fmars.2018.00095.

Savchuk, O.P., Gustafsson, B.G., Müller-Karulis, B., 2012. BALTSEM - a marine model for decision support within the Baltic Sea region. In: BNI Technical Report No. 7.

Schneider, B., 2011. The CO_2 system of the Baltic Sea: biogeochemical control and impact of anthropogenic CO_2. In: Global Change and Baltic Coastal Zones, Coastal Research Library. Springer, Dordrecht, pp. 33–49. https://doi.org/10.1007/978-94-007-0400-8_3.

Stigebrandt, A., Gustafsson, B.G., 2003. Response of the Baltic Sea to climate change—theory and observations. J. Sea Res. 49, 243–256. https://doi.org/10.1016/S1385-1101(03)00021-2.

Sun, X., Mörth, C.-M., Humborg, C., Gustafsson, B.G., 2017. Temporal and spatial variations of rock weathering and CO_2 consumption in the Baltic Sea catchment. Chem. Geol. 466, 57–69. https://doi.org/10.1016/j.chemgeo.2017.04.028.

Ulfsbo, A., Kuliński, K., Anderson, L.G., Turner, D.R., 2015. Modelling organic alkalinity in the Baltic Sea using a Humic-Pitzer approach. Mar. Chem. 168, 18–26. https://doi.org/10.1016/j.marchem.2014.10.013.

van Vuuren, D.P., Edmonds, J., Kainuma, M., Riahi, K., Thomson, A., Hibbard, K., Hurtt, G.C., Kram, T., Krey, V., Lamarque, J.-F., Masui, T., Meinshausen, M., Nakicenovic, N., Smith, S.J., Rose, S.K., 2011. The representative concentration pathways: an overview. Climatic Change 109 (5). https://doi.org/10.1007/s10584-011-0148-z.

Weiss, R.F., 1974. Carbon dioxide in water and seawater: the solubility of a non-ideal gas. Mar. Chem. 2, 203–215. https://doi.org/10.1016/0304-4203(74)90015-2.

Wolf-Gladrow, D.A., Zeebe, R.E., Klaas, C., Körtzinger, A., Dickson, A.G., 2007. Total alkalinity: the explicit conservative expression and its application to biogeochemical processes. Mar. Chem. 106, 287–300. https://doi.org/10.1016/j.marchem.2007.01.006.